



Impacts of climate change on meteorological and hydrological drought in the Casamance basin in Kolda and the Kayanga basin in Wassadou

Sadio C. A. A S.¹, Faye C.², Dione P.M.³

¹Department of Geography, U.F.R. Sciences and Technologies, Assane Seck University of Ziguinchor, Geomatics and Environment Laboratory, BP 523 Ziguinchor (Senegal),

²Department of Geography, U.F.R. Sciences and Technologies, Assane Seck University of Ziguinchor, Geomatics and Environment Laboratory, BP 523 Ziguinchor (Senegal),

³Department of Geography, U.F.R. Sciences and Technologies, Assane Seck University of Ziguinchor, Geomatics and Environment Laboratory, BP 523 Ziguinchor (Senegal),

**Cheikh Abdoul Aziz Sy Sadio, Email address: C.SADIO4153@zig.univ.sn

*Cheikh Faye, Email address: cheikh.faye@univ-zig.sn

*Philippe Malick Dione, Email address: pm.d11@zig.univ.sn

Received 22 Dec 2023,
Revised 14 Jan 2024,
Accepted 16 Jan 2024

Keywords:

- ✓ drought;
- ✓ climate change,;
- ✓ projection;
- ✓ scenario;
- ✓ watershed

Citation: Sadio C. A. A S., Faye C., Dione P. M., (2024) Impacts of climate change on meteorological and hydrological drought in the Casamance basin in Kolda and the Kayanga basin in Wassadou, *J. Mater. Environ. Sci.*, 15(1), 83-115

Abstract: As in many other African countries, the incidence of drought is increasing in Senegal. In this work, the spatio-temporal changes of droughts under different SSP (Shared Socio-economic Pathways) scenarios were evaluated; given their greatest impacts on people's lives and livelihoods, particularly when droughts coincide with crop growing seasons. From a set of high-performance general circulation models (GCM), temperature precipitation data over the future period (2021 to 2100) within the framework of the CMIP6 climate scenarios (SSP 126 and SSP 585) in the basins from Casamance to Kolda station and Kayanga to Wassadou station. Two meteorological drought indices, including the standardized precipitation index (SPI) and the standardized precipitation and evapotranspiration index (SPEI) and a hydrological drought index, the standardized flow index (SSI), are evaluated at different time scales from the monthly average of precipitation, temperature and flow projected by GCM in order to predict possible spatio-temporal changes in meteorological droughts. Finally, the trends of SPEI, SPI and SSI, and drought characteristics at monthly scale were estimated using an 80-year moving window, with an interval of 10 years, to understand the drivers' determinants responsible for future changes in droughts. The results indicated a decrease in precipitation and an increase in temperature for both basins. This decrease in precipitation accompanied by an increase in temperature would reduce the SPEI, SPI and SSI across the two basins, which would make droughts more frequent under both scenarios (SSP 126 and SSP 585). However, the increase in drought frequency would be less for SSP 126, compared to SSP 585, due to the stability of temperature and the small decrease in precipitation towards the end of the century.

1. Introduction

In the context of global warming, extreme weather and climate events such as floods and drought appear to be occurring more frequently. Drought, generally defined as a deficit of water over a specified period (Törnros and Menzel, 2014), is one of the most costly and widespread natural disasters with negative impacts on agriculture, water resources, natural ecosystems and societal activities (Du et al.,

2013, Sahoo *et al.*, 2015). Droughts are oPETn divided into four categories according to the American Meteorological Society (Council, 2004, Benitez and Domecq, 2014): (1) Meteorological drought is defined as a lack of precipitation over a region during a given period. (2) Agricultural drought refers to a period characterised by a lack of moisture in the soil, leading to a reduction in crop production and plant growth (3) Hydrological drought occurs when surface and groundwater resources are insufficient; (4) Socio-economic drought is associated with an insufficient supply of water resources to meet the economic demand associated with the above three types of drought. Studies have pointed to the continuation or intensification of changes in climate hazards in the future (Salman *et al.*, 2015, Shiru *et al.*, 2020). Therefore, it is imperative to understand future climate variations in order to develop appropriate mitigation and adaptation measures to reduce the risk of damage and loss of life and property. It is also necessary to monitor meteorological drought in a timely manner and implement early warning and risk management of water resources and agricultural production (Zhang and Jia, 2013; Xing *et al.*, 2015; Mdehheb *et al.*, 2020).

Drought is an extremely devastating natural hazard that is expected to increase in many parts of the world due to greater climate variability (Rashid *et al.*, 2015, Sa'adi *et al.*, 2017). Although droughts are classified as meteorological, agricultural, hydrological and socio-economic, meteorological droughts precede and exacerbate all other drought types (Potop *et al.*, 2014) and, therefore, understanding them is crucial for developing mitigation measures. This occurs due to a reduction in precipitation or atmospheric water balance relative to the long-term average. Meteorological drought is accompanied by below-normal precipitation and above-normal temperatures. Therefore, it can occur in any climate regime due to natural climate variability (Mishra and Singh, 2010). Increased climate variability due to global warming has increased the frequency and severity of droughts in many parts of the world in recent decades (Sung and Chung, 2014, Mohsenipour *et al.*, 2018), which are expected to swell with global warming.

The African continent is considered to be highly prone to droughts due to the high variability of rainfall. A large number of extreme droughts have been observed in the recent past, causing famine and the loss of millions of lives in Africa (Masih *et al.*, 2014). Studies have reported a more erratic behaviour of the climate due to climate change, and therefore potentially an increase in its severity in different countries, including Senegal (Faye *et al.*, 2015, Faye *et al.*, 2017, Faye, 2017 & 2018). Numerous studies on climate variability and the changing nature of droughts using various indices have been conducted in Senegal (Faye *et al.*, 2015, Faye *et al.*, 201, Faye, 2017 & 2018). Although major drought episodes have not occurred in Senegal in recent decades, studies have shown an upward trend in climate variability and, consequently, a potential increase in the frequency of droughts and the areas affected (Faye, 2017 & 2018). Continuation of the current drought trend may have serious social, environmental and economic consequences for the country (Shiru *et al.*, 2020). It would be very devastating if it continued to occur during crop growing seasons, as the economy and livelihoods of the majority of the population depend heavily on rain-fed agriculture.

A large number of general circulation models (GCMs) are publicly available in phase 6 of the Coupled Model Intercomparison Project (CMIP6), which have been widely used for drought projections. The CMIP6 GCMs are available at a finer resolution than the CMIP5 GCMs, and can be used directly at local level. These models produce better quality, higher resolution estimates of regional climate change for all regions of the world. It provides access to various historical data and potential future scenarios of radiative forcing dependent on greenhouse gas emissions (Carvalho *et al.*, 2020). These scenarios, known as SSPs (Shared Socioeconomic Pathways), contain specific descriptions of the future population, economy, technological development, lifestyle, policies and other social factors.

In general, they offer five different possibilities by which the future world can meet the challenges of climate change in terms of adaptation and mitigation (O'Neill *et al.*, 2015) and provide a means of examining the possible challenges associated with climate change adaptation and mitigation (Chen *et al.*, 2020).

Although climate projections for Senegal have been assessed in a number of studies (Mbaye *et al.*, 2019, Sadio *et al.*, 2020, Diakhaté *et al.*, 2022), their impacts on droughts have not been taken into account, particularly during the different seasons of and using a set of CMIP6 models. Various indices have been used in different parts of the world to assess droughts. These include the Standardised Precipitation and Evapotranspiration Index (SPEI) (Vicente-Serrano *et al.*, 2010), the Standardised Precipitation Index (SPI) (McKee *et al.*, 1993) and the Standardized Streamflow Index (SSI) (Barker *et al.*, 2016, Wang *et al.*, 2020) have proven to be very effective, mainly for semi-arid environments due to the inclusion of potential evapotranspiration (PET) in the drought estimation, a factor of paramount importance for these regions (Begueria *et al.*, 2019).

The main objective of this study was to project future changes in meteorological and hydrological drought during the growing seasons in the Casamance river basins at the Kolda station and the Kayanga at the Wassadou station.

2. Study area

The Casamance basin, which extends over three administrative regions (Ziguinchor, Sédhiou and Kolda) in southern Senegal, lies between 12°20' and 13°21' north latitude and 14°17' 1 and 16°47' west longitude (Map 1). The basin covers an area of around 20150 km², stretching 270 km from west to east and 100 km from north to south (Dacosta, 1989). The climate in Casamance is Atlantic Sudanian and Southern Sudanian (Sané *et al.*, 2011), and is strongly influenced by geographical and atmospheric factors (Sagna, 2005). From a topographical point of view, the Casamance watershed is characterised by its low relief. In fact, all the rivers have their source on the terminal continental plateau. The shallowness of the slopes explains the deep invasion of the sea into the Casamance basin, resulting in the salinisation of farmland (PADERCA, 2008). The Casamance watershed upstream of Kolda has a surface area of 3,650 km², with a maximum altitude of 80 m and a minimum altitude of 10 m.

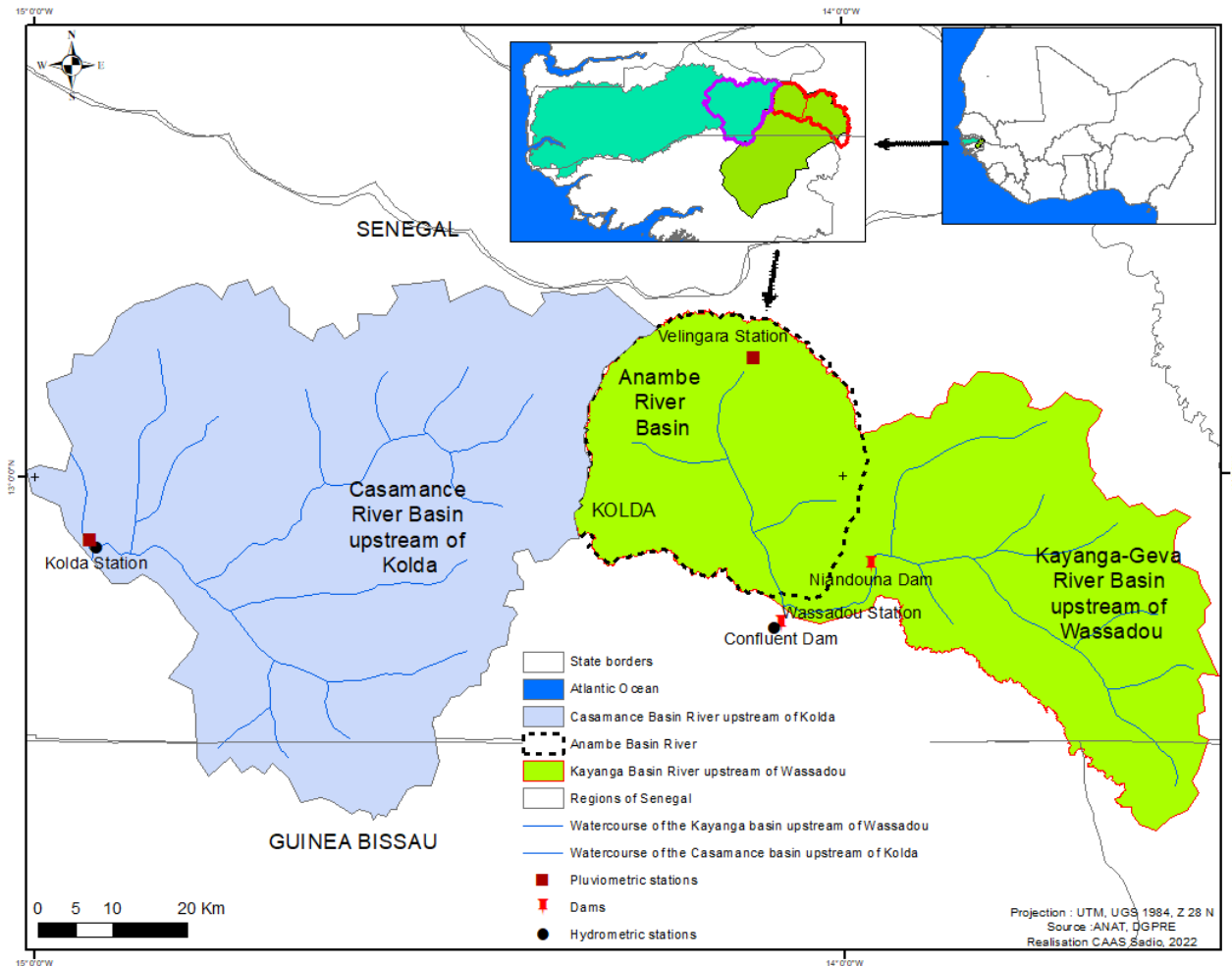
The Kayanga-Geba catchment is a transboundary basin shared by three countries, Guinea, Senegal and Guinea-Bissau. It lies between latitudes 12°31 and 13°09 N and longitudes 13°20 and 14°26 W, in the south of Senegal and the north of Guinea-Bissau. It is bounded to the east by the Koulountou watershed, a left-bank tributary of the Gambia, and to the west by the Casamance watershed. The Kayanga/Geba basin covers an area of 10,325 km² at the Bafata station in Guinea-Bissau and 1,640 km² at the border between Senegal and Guinea-Bissau. Since the 1970s, a sharp drop in groundwater levels throughout the basin has had a serious impact on low-water flows. The Kayanga Géva basin upstream of Wassadou covers an area of 3,163 km² and includes the Anambé sub-basin (OMVG, 2012). The Anambé is a tributary of the Kayanga that drains a catchment area of 1,100 km² with a valley floor consisting of hydromorphic soils that flood for three to four months (OMVG, 2012). It drains a basin used as a reservoir for the dam located 300 m downstream of the confluence dam on Senegalese territory, with a reserve of around 50 million m³.

3. Methodology

3.1 Data

The latest CMIP6 simulations presented in the IPCC's 6th Assessment Report were used for the climate projections. Eighteen (18) climate models were used. The ensemble mean of these models was

calculated for the analyses, which reduces the natural variability and systematic biases present in individual models (Akinsanola and Zhou, 2019). Data were corrected using the modified quantile method (Bai *et al.*, 2016). The precipitation and temperature data in this study area extracted from the models were used in the GR2M model to simulate the runoff data also used in this study. In this study, we worked mainly with the SSP 126 (low adaptation challenge, low mitigation challenge) and SSP 585 (high mitigation challenge) scenarios (Gidden *et al.*, 2019) and the future data are selected over the period 2021-2100.



Map 1. Geographical location of the Casamance at the Kolda station and the Kayanga at the Wassadou station.

3.2 Assessment of drought indices

3.2.1. Meteorological drought indices

Two drought indices are used in this study, namely the Standardised Precipitation Index (SPI) (McKee *et al.*, 1993) and the Standardised Precipitation and Evapotranspiration Index (SPEI) (Vicente-Serrano *et al.*, 2010) to characterise meteorological drought. These indices are calculated at different time scales on the basis of monthly precipitation (P) and potential evapotranspiration (PET) data. In this study, time scales of 1, 3, 6, 12 and 24 months were used as accumulation periods for monitoring drought events. These different time scales are chosen to reflect the impacts of precipitation deficits on different types of water resources. The SPI uses accumulated precipitation, while the SPEI is assessed from climatic water balance values, estimated as the accumulated difference between precipitation and PET over the selected time scale.

3.2.1.1. SPEI

The SPEI is considered an improved drought index, particularly suitable for analysing the effect of global warming on drought conditions (Beguería et al., 2015). The calculation of the SPEI in this study follows the method mentioned in the study by (Vicente-Serrano et al., 2010). The SPEI is based on a climatic water balance that is determined by the difference between Precipitation (P) and Potential Evapotranspiration (PET) for month i:

$$D_i = P_i - ETP_i \quad (12)$$

D_i provides a simple measure of the water surplus or deficit for the month analysed. PET is calculated using the Thornthwaite equation (Thornthwaite, 1948).

The values calculated D_i are aggregated at different time scales, using the same procedure as for the SPI. The difference $D_{i,j}^k$ in a given month j and year i depends on the time scale chosen, k. For example, the difference accumulated during one month of a given year, with a time scale of 12 months, is calculated according to the following formula:

$$X_{i,j}^k = \sum_{l=13-k+j}^{12} D_{i-l,j} + \sum_{l=1}^j D_{i,l,j}, \quad si \ j < k, et \quad (13)$$

$$X_{i,j}^k = \sum_{l=j-k+j}^j D_{i,l,j}, \quad si \ j \geq k \quad (14)$$

Where $D_{i,j}$ is the difference in P-PET for the first month of year i, in mm.

Next, the log-logistic distribution is selected to normalise the D series in order to obtain the SPEI. The probability density function of the log-logistically distributed variable is expressed as follows:

$$f(x) = \frac{\beta}{\alpha} \left(\frac{x-\gamma}{\alpha}\right)^{\beta-1} \left[1 + \left(\frac{x-\gamma}{\alpha}\right)^{\beta}\right]^{-2} \quad (15)$$

Where α , β and γ are the scale, shape and origin parameters respectively for D values within the range ($\gamma > D < \infty$).

The probability distribution function of series D is given by:

$$F(x) = \left[1 + \left(\frac{\alpha}{x-\gamma}\right)^{\beta}\right]^{-1} \quad (16)$$

With $F(x)$, the SPEI can easily be obtained as normalized values of $F(x)$. For example, following the classical approximation of Abramowitz and Stegun (1965):

$$SPEI = W - \frac{C_0 + C_1 W + C_2 W^2}{1 + d_1 W + d_2 W^2 + d_3 W^3} = \quad (17)$$

Where $W = \sqrt{-2 \ln(p)}$ for $p \leq 0.5$ and p is the probability of exceeding a given value D, $p = 1 - F(x)$. If $p > 0.5$, p is replaced by $1 - p$ and the sign of the resulting SPEI is reversed. The constants are: $C_0 = 2.515517$, $C_1 = 0.802853$, $C_2 = 0.010328$, $d_1 = 1.432788$, $d_2 = 0.189269$ and $d_3 = 0.001308$. Positive SPEI values indicate above-average humidity conditions, while negative values indicate drought conditions. A drought event is defined when the SPEI value is less than or equal to -1 over a certain period.

3.2.1.2. SPI

The SPI is a probability index derived solely from rainfall statistics for a certain location and period (months or years). This index converts the cumulative probability into the standard normal random variable (Van Vuuren et al., 2011). The median precipitation value and the SPI quantify the probability of observing a given amount of precipitation in a certain period of time (Saada et al., 2017). Negative and positive SPI values indicate dry and wet conditions, respectively; these values become more negative or positive, respectively, as dryness or wetness increases (Butu et al., 2020). In this study, three-month (SPI 3) (January-March), six-month (SPI 6) (January-June) and twelve-month (SPI 12) (January-December) SPIs were used to describe, respectively, seasonal changes in precipitation, changes corresponding to agricultural drought, annual changes and longer-term trends corresponding to hydrological drought (Zeybekoğlu et al., 2021). The dataset has evolved, and a new SPI value is added each month, derived from the values calculated in previous months. The probability of any observed precipitation data point was calculated from the historical records. This probability was used in conjunction with an inverse normal estimate to calculate the deviation of precipitation from a normally distributed probability density with mean zero and standard deviation unity. This number was the SPI for the rainfall data point (Javanmard et al., 2017). Given a normal distribution function with zero mean and variance, the SPI was calculated as follows (Fung et al., 2019) :

For $0 < H(x) \leq 0.5$,

$$SPI = - \left(t - \frac{c_0 + c_1 + c_2 + t^2}{1 + d_1 t + d_2 t + d_3 t} \right), \quad t = \sqrt{\ln \frac{1}{(H(x))^2}} \quad (10)$$

For $0.5 < H(x) \leq 1$,

$$SPI = + \left(t - \frac{c_0 + c_1 + c_2 + t^2}{1 + d_1 t + d_2 t + d_3 t} \right), \quad t = \sqrt{\ln \frac{1}{(1,0-H(x))^2}} \quad (11)$$

where $c_0 = 2,515517$, $c_1 = 0,802853$, $c_2 = 0,010328$, $d_1 = 1,432788$, $d_2 = 0.189269$ and $d_3 = 0.001308$ (Javanmard et al., 2017)

3.2.2 Hydrological drought index

To assess or monitor HD in NRUW, the Standardised Flow Index (SSI) proposed by (Vicente-Serrano et al., 2012) was used in this study. For the SSI calculations, the procedure was similar to that of the SPI/SPEI. The Gamma distribution function was selected as the most appropriate distribution function to calculate the SSI (Wang et al., 2020, Salimi et al., 2021). Based on the index values (SPI or SPEI or SSI), meteorological and hydrological drought states are defined. Five states are considered, designated by an integer ranging from 0 (no drought) to 4 (extreme drought) and defined using the criteria in Table 1.

Table 1. Categorisation of the degree of drought/humidity based on standardised precipitation and evapotranspiration indices

SPEI values	Sequences of droughts	SPEI values	Wet sequences
$SPEI < -2.00$	Extremely dry	$2.00 < SPEI$	Extremely humid
$-1.50 < SPEI < -2.00$	Severely dry	$1.50 < SPEI < 2.00$	Severely damp
$-1.00 < SPEI < -1.50$	Moderately dry	$1.00 < SPEI < 1.50$	Moderately humid
$0.00 < SPEI < -1.00$	Slightly dry	$0.00 < SPEI < 1.00$	Slightly damp

3.3. Analysis of drought intensity using cycle theory

Drought characteristics include various drought conditions, such as duration, severity and intensity. A probabilistic methodology widely used in the characterisation of drought is the application of cycle theory (Yevjevich, 1967), which makes it possible to estimate the return periods of extreme events (González and Valdés, 2006). Cycle theory has been applied to analyse the characteristics of drought on the basis of SPEI, SPI and SSI. Figure 1 shows the drought characteristics using run theory for a given threshold level. An analysis is defined as a part of the time series of a drought variable, in which all values are below or above the selected truncation level. Consequently, it is called either a negative or a positive run (Mishra and Singh, 2010). Theoretically, drought intensity is the average value of a drought parameter below the threshold, which is measured by dividing drought severity by duration (Lee et al., 2017). In this study, we defined the SPEI (SPI or SSI) equal to -1 as the threshold value for identifying drought conditions, with SPEIs (SPI or SSI) lower than -1 being used to estimate drought intensity (Bae et al., 2018).

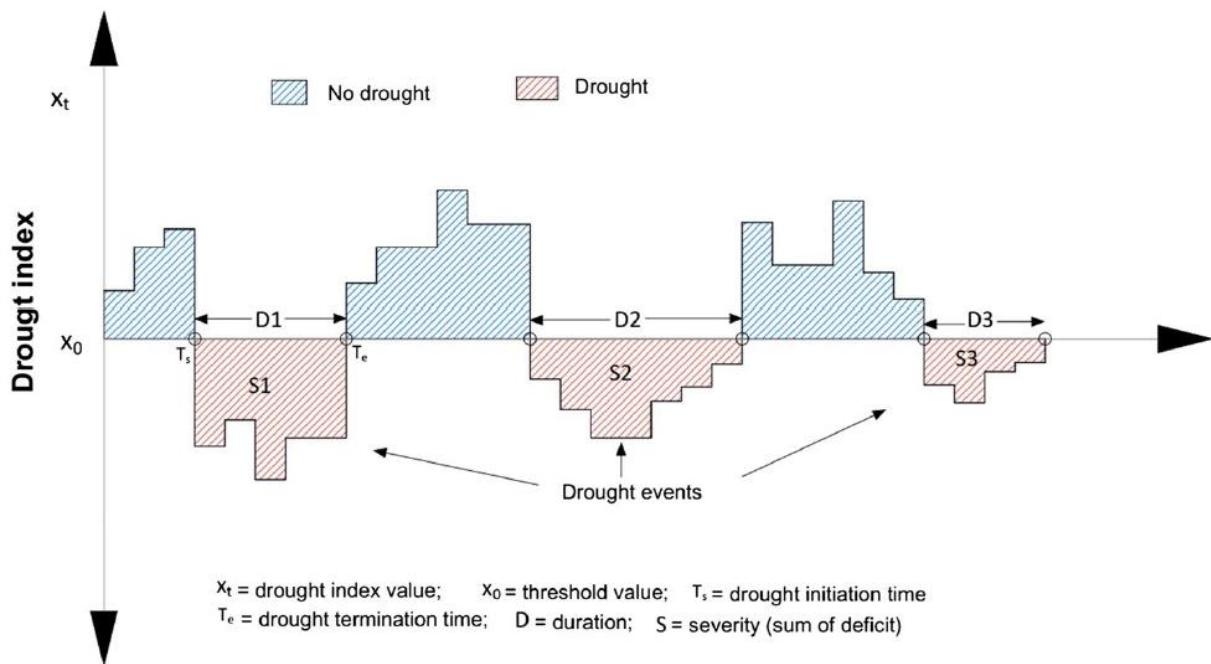


Figure 1. Drought characteristics above a given threshold level Source: (Lee et al., 2017)

3.4. Analysis of drought trends

3.4.1. Pettitt test (1979)

A break is defined as a change in the probability distribution of the random variables whose successive realisations define the time series studied (Servat et al., 1998). The Pettitt test was chosen for its power and robustness (Lubès-Niel et al., 1998). The Pettitt test is a non-parametric test for detecting a single break at an unknown date. The Pettitt variable ($U_{t,N}$) is defined by equation 10.

$$U_{t,N} = \sum_{i=1}^t \sum_{j=t+1}^N D_{ij} \quad (10)$$

With

$$S = \sum_{i=1}^k \sum_{j=k+1}^n \text{signe}(x_j - x_i) \quad (11)$$

If the null hypothesis is rejected, an estimate of the break date is given by the time t defining the maximum in absolute value of the variable U_t , N (Soro et al., 2011). Note that the test also provides an estimate of the position of the break using the index k corresponding to the maximum $U(k)$. The hydrological deficit in relation to the breaks identified by the Pettitt test was evaluated using equation 12 (Ardoin, 2004):

$$D = \frac{X_j}{X_i} - 1 \quad (12)$$

Where X_j is the average of the series $aPET_r$ the break and \bar{X}_i that before the break.

3.4.2. Mann-Kendall test

The Mann-Kendall test was used to detect any gradual changes in the series of extreme variables. According to Mann (1945) and Kendall (1975), this non-parametric test, based on rank, can be used to determine whether the correlation between time and the study variable is significant or not. Let (x_1, \dots, x_n) be a sample of independent values relating to a random variable X whose stationarity is to be assessed. The Mann-Kendall statistic is defined as follows:

$$S = \sum_{i=1}^{n-1} \sum_{j=i+1}^n \text{signe}(x_i - x_j) \quad (13)$$

To determine the magnitude of the change, the Sen slope method (Sen, 1968) was applied and is obtained by the following formula (Equation 14):

$$b = \text{Mediane} \left[\frac{(X_j - X_i)}{(j - i)} \right], \text{ pour } i < j \quad (14)$$

Where b is the slope between the data points X_j and X_i measured at time j and i respectively.

3.5. Multi-scale analysis of teleconnections between meteorological and hydrological droughts

3.5.1 Correlation analysis

Correlation analysis was performed to determine the correlations between MD and HD on time scales of 1, 3, 6, 12 and 24 months. Thus, the Pearson correlation coefficient (PCC) and the cross-correlation function (CC), which have been widely used in hydrological research (Ma et al., 2019, Wang et al., 2020) were used in this study to estimate the correlation coefficients between SPI and Time Series SSI, SPEI and SSI at the 5% significance level (Lorenzo-Lacruz et al., 2013, Huang et al., 2016, Wang et al., 2020, Jehanzaib et al., 2023). The CC ranges from -1 to 1 with a $CC > 0$ indicating a positive linear correlation and a $CC < 0$ indicating a negative linear correlation. Furthermore, the closer the CC is to 1 or -1, the stronger the linear correlation (da Silva et al., 2016, Wu et al., 2018). CC has also been used to study the propagation time of meteorological drought and hydrological drought (Barker et al., 2016, Wang et al. 2020). CCF ranges from -1 to 1. In this study, the propagation of drought from MD to HD is characterised by a lag (Salimi et al., 2021).

3.5.2. Relationship between meteorological and hydrological drought

Based on the correlation between SPEI-SSI and SPI-SSI previously identified, the relationship between hydrological and meteorological drought characteristics was established using non-linear models (power, exponential and logarithmic) (Wu et al., 2017, Salimi et al., 2021, Jehanzaib et al., 2023, Fowé et al., 2023). The coefficient of determination (R^2) (Draper and al., 1998) was evaluated to assess the amount of variance explained in each case and thus select the optimal nonlinear model.

4. Results and Discussion

4.1 Variations in annual precipitation, PET, flow and water balance

The results of the Pettitt tests are presented in **Table 1**. In the Casamance basin at the Kolda station, over the period 2021-2100, a decrease in rainfall would be noted for the SSP 126 and SSP 585 scenarios. This downward trend is confirmed by the Pettitt test (**Table 1**), which shows a break in the rainfall series in 2065 and 2051 respectively for the SSP 126 and SSP 585 climate change scenarios over the study period (2021-2100). On either side of the break date, a decrease of around 4.59 and 23.7% respectively for the SSP 126 and SSP 585 climate change scenarios. In the Kayanga basin at Wassadou, the disruption will clearly occur on the same dates (2065 for SSP 126 and 2051 for SSP 585), with rainfall decreasing on either side of the disruption dates by 3.4% and 21.6% respectively under SSP 126 and SSP 585 (**Figure 2**).

Table 1. Pettitt test on the SPEI and SPI per scenario for the period 2021-2100 in the Casamance basin in Kolda and the Kayanga basin in Wassadou

	Kolda				Wassadou			
SSP 245	Pmm	PET	P-PET	Flow	Pmm	PET	P-PET	Flow
Termination date	2065	2056	2055	2053	2065	2055	2055	2065
p-value	0,012	< 0,0001	< 0,0001	< 0,0001	0,053	< 0,0001	< 0,0001	0,000
Average before break	591	2379	-1783	2,87	617	2649	-2032	0,003
Average aPETr breakage	565	2590	-2014	2,41	596	2881	-2281	0,003
Rate of change	-4,59	+8,16	+11,5	-19,05	-3,4	+8,05	+10,9	-23,5
SSP 585	Pmm	PET	P-PET	Flow	Pmm	PET	P-PET	Flow
Termination date	2051	2056	2058	2052	2051	2058	2058	2056
p-value	< 0,0001	< 0,0001	< 0,0001	< 0,0001	< 0,0001	< 0,0001	< 0,0001	< 0,0001
Average before break	645	2379	-1773	3,39	662	2465	-1816	0,005
Average aPETr rupture	524	3828	-3352	1,49	544	3986	-3448	0,001
Rate of change	-23,07	+37,9	+47,1	-127	-21,6	+38,2	+47,3	-308

For the 2030 climate horizon (2021-2040 period), precipitation should increase slightly, as indicated for the SSP 126 and SSP 585 scenarios, by around -0.147 and 0.021 mm per year, respectively. On the other hand, for the 2050 (2041-2060) and 2070 (1961-2080) horizons, a decrease in precipitation would also be noted under the SSP 126 and SSP 585 scenarios. This decrease would be of the order of -0.147 mm per year for the SSP 126 scenario and -0.505 mm per year for the SSP 585 scenario over the 2050 horizon (2041-2060), and of the order of -0.274 mm per year for the SSP 126 scenario and -0.116 mm per year for the SSP 585 scenario over the 2070 horizon (1981-2100). For the 2090 horizon (1981-2100), the situation would be disparate, with an increase of around 0.158 mm per year for the SSP 126 scenario, while for the SSP 585 scenario, a decrease in precipitation of around -0.295 mm per year would be noted. The decrease in rainfall is confirmed in the Kayanga basin upstream of Wassadou (**Table 1**).

Analysis of the series shows an upward trend in temperatures and hence in potential evapotranspiration (PET) over the period 2021-2100, with a break noted in 2056 for the SSP 126 and SSP 585 scenarios at the Kolda station, and in 2055 and 2058 for the SSP 126 and SSP 585 scenarios at the Wassadou station (**Table 1**). On either side of the break-up date, an increase in PET will be of the order of 8.16 and 37.9% respectively for the SSP 126 and SSP 585 scenarios. For the Kayanga basin at the Wassadou station, the post-disruption increase will be of the order of 8.05% under SSP 126 and 38.2% under SSP 585.

This trend towards increasing temperatures and potential evapotranspiration, accompanied by decreasing rainfall, results in a decrease in runoff with a break that will occur in 2053 and 2052 respectively under the SSP 126 and SSP 585 scenarios at the Kolda station, and in 2065 and 2056 for the SSP 126 and SSP 585 scenarios at the Wassadou station (Table 1). On either side of the break-up date, a fall in runoff will be of the order of 19.05 and 127% respectively for the SSP 126 and SSP 585 scenarios. For the Kayanga basin at the Wassadou station, the drop aPETr the rupture will be of the order of 23.5% under SSP 126 and 308% under SSP 585.

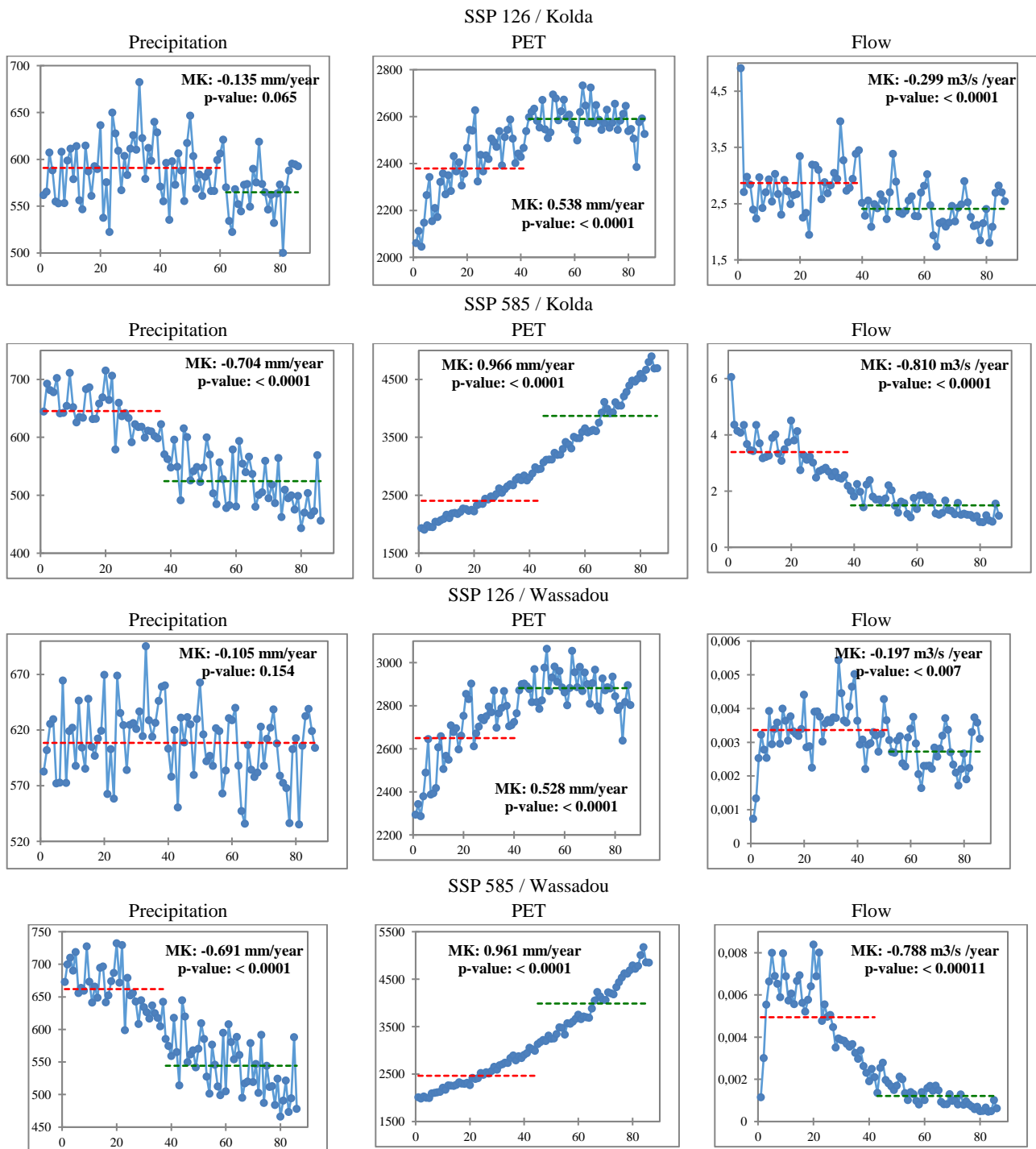


Figure 2. Detection of breakpoints in the annual hydrological time series (rainfall, PET and discharge by scenario over the period 2021-2100 in the Casamance basin in Kolda and the Kayanga basin in Wassadou).

Compared with the historical period (1985-2014), a general decrease in rainfall and a general increase in temperature over the four horizons studied would be noted in the Casamance basin at Kolda. This decrease in rainfall over the 2030, 2050, 2070 and 2090 climate horizons, compared with the historical period, could reach values of 7.90, 6.11, 9.25 and 10.97% respectively in the SSP 126 scenario, and 7.77, 16.31, 22.15 and 11.04% respectively over the 2050, 2070 and 2090 horizons in the SSP 585 scenario. Temperatures could rise by a record 2.09°C over the period 2061-2080 in the SSP 126 scenario and 5.20°C over the period 2081-2100 in the SSP 585 scenario. The Mann Kendall trend test was used to estimate the trends and magnitude of changes in the time series of hydrological variables. **Figure 2** shows the results of the test for annual precipitation, PET and flow, respectively. Annual precipitation and discharge showed a decreasing trend, while PET showed a statistically significant increasing trend (p-value < 0.05) from 2021 to 2100. At the Kolda station (**Figure 2**), this decrease in precipitation will be -0.115 mm per year and -0.704 mm per year for the SSP 126 and SSP 585 scenarios respectively. For runoff, the decrease will be of the order of -0.299 m³/s per year and -0.810 m³/s per year for the SSP 126 and SSP 585 scenarios respectively. As for PET, its increase will be of the order of -0.558 mm per year and -0.966 mm per year for the SSP 126 and SSP 585 scenarios respectively. Trends of decreasing rainfall and discharge and decreasing PTE will also be noted in the Kayanga basin at the Wassadou station.

4.2 Temporal changes in drought indices and trend analysis

Mean rainfall and temperature were used to estimate future changes in drought in the Casamance basin at the Kolda station and the Kayanga basin at the Wassadou station. The projection of climate and hydrology in these basins revealed significant changes in precipitation and temperature for different SSPs. The temporal patterns of trends in the IPDS, SPI and SSI on different scales (1, 3, 6, 12 and 24 months) from 2021 to 2100 are shown in **Figures 1, 2, 3 and 4** for SSP 126 and SSP 585 in the Casamance basin at Kolda and the Kayanga basin at Wassadou. Given the trend in precipitation, which would vary considerably for the different seasons, and the increase in temperature, the SPEI, SPI and SSI would decrease over the whole of the two basins for the different scales. The magnitude of changes in the SPEI, SPI and SSI was found to vary considerably due to the wide variation in temperature, precipitation and flow. Fluctuations in drought index values on different time scales may reflect variations in drought. The drought variations to be observed seem more pronounced on shorter time scales (1, 3 and 6 months). The cumulative effects of SPI, SPEI and SSI become striking and clearer with longer dry (**Figures 1, 2, 3 and 4**, red) and wet (**Figures 1, 2, 3 and 4**, blue) periods as the time scale increases (Fowé et al., 2023). On the basis of the longer time-scale SPI and SPEI values, the driest period would be observed in the 2050s in the study area, and would be more pronounced under the SSP 585 scenario than under the SSP 126 scenario. This is consistent with the climate projections and simulations of CMIP 6 (Coupled Model Intercomparison Project 6) during the 21st century insofar as SSP126 and SSP585 are the CMIP6 scenarios with respectively the lowest and highest values in terms of anthropogenic radiative forcing by 2100, global CO₂ concentration, global CO₂ emissions, with socio-economic reasons (Wan Zunairah and coauthors., 2023).

Changes in drought are expected to be most pronounced in these two basins located in the humid and semi-humid regions of Senegal in the medium and distant future. These changes would be significant at the end of the 21st century under higher emissions scenarios (SSP 585). Similarly, such changes have also been observed in the temporal patterns of changes in drought or humidity. As shown in **Figures 2, 3, 4 and 5**, significant changes in drought are expected to be dominant in most networks in the Casamance basin at the Kolda station and the Kayanga basin at the Wassadou station.

The reduction in the SPEI should be slightly higher in the Casamance basin at the Kolda station than in the Kayanga basin at the Wassadou station (**Table 2**). The contrast remains apparent between the first two sub-periods (2021-2040 and 2041-2060), which tend to be wet, and the last two (2061-2080 and 2081-2100), which tend to be dry. The percentage of dry years at all scales over the 2081-2100 period averages 78.02% under SSP 126 and 94.6% under SSP 585 in the Casamance basin at the Kolda station, and 73.2% under SSP 126 and 94.9% under SSP 585 in the Kayanga basin at the Wassadou station. For the SPI, it is declining and varies on average from 65.8% under SSP 126 and 86.5% under SSP 585 at the Kolda station, and from 57.9% under SSP 126 and 85.8% under SSP 585 at the Wassadou station. Finally, for the SSI, this percentage of dry years at all scales towards the end of the century averages 76.8% under SSP 126 and 100% under SSP 585 at the Kolda station, and 100% under SSP 126 and SSP 585 at the Wassadou station, indicating the widespread nature of the hydrological drought towards the end of the century in these basins.

Table 1. Statistics on drought sequences on the SPEI, SPI and SSI by scenario over the period 2021-2100 in the Casamance basin in Kolda and the Kayanga basin in Wassadou.

KOLDA	SSP 126					SSP 585				
	SPEI 1	SPEI 3	SPEI 6	SPEI1 2	SPEI2 4	SPEI 1	SPEI 3	SPEI 6	SPEI1 2	SPEI2 4
2021-2040	35,8	30,8	29,2	28,3	21,3	15,8	10,0	3,3	0,0	0,0
2041-2060	41,3	35,8	29,2	27,5	18,8	41,7	38,3	32,1	22,9	26,3
2061-2080	56,7	60,4	65,4	72,1	80,8	65,4	73,3	83,3	90,8	99,2
2081-2100	68,8	74,2	79,6	79,2	88,3	83,8	92,9	96,3	100	100
SPI	SPI1	SPI3	SPI6	SPI12	SPI24	SPI1	SPI3	SPI6	SPI12	SPI24
2021-2040	52,5	48,8	46,3	43,8	46,3	31,7	24,2	12,1	0,0	0,0
2041-2060	48,8	41,3	35,8	30,0	22,5	47,5	44,2	37,9	29,2	32,5
2061-2080	48,3	47,5	52,1	53,8	52,9	56,7	64,2	71,7	86,7	91,3
2081-2100	54,6	58,8	66,3	72,5	77,1	71,3	76,3	85,4	99,6	100
SSI	SSI1	SSI3	SSI6	SSI12	SSI24	SSI1	SSI3	SSI6	SSI12	SSI24
2021-2040	38,8	39,6	38,3	37,9	32,1	0,0	0,0	0,0	0,0	0,0
2041-2060	25,4	25,0	26,7	29,6	26,3	25,4	26,7	26,7	26,7	30,8
2061-2080	55,0	55,4	57,1	59,6	65,0	92,1	92,5	93,3	96,3	100
2081-2100	73,3	75,4	77,5	79,6	78,3	100	100	100	100	100
WASSADOU	SSP 126					SSP 585				
SPEI	SPEI1	SPEI3	SPEI6	SPEI12	SPEI24	SPEI1	SPEI3	SPEI6	SPEI12	SPEI24
2021-2040	35,0	30,0	27,5	26,3	17,5	15,0	7,1	2,5	0,0	0,0
2041-2060	45,4	39,6	35,0	28,3	27,9	41,3	38,3	32,1	23,3	26,7
2061-2080	58,8	62,1	65,4	71,3	84,2	67,1	74,6	81,7	93,8	97,9
2081-2100	65,0	72,5	75,4	75,0	78,3	85,8	92,1	96,7	100	100
SPI	SPI1	SPI3	SPI6	SPI12	SPI24	SPI1	SPI3	SPI6	SPI12	SPI24
2021-2040	51,7	49,2	47,5	47,5	37,9	30,0	21,7	11,7	0,0	0,0
2041-2060	48,3	45,0	37,9	23,3	28,8	46,7	44,2	39,2	29,2	30,8
2061-2080	49,2	49,2	49,6	52,1	59,6	57,9	65,8	73,8	86,7	91,3
2081-2100	52,1	53,8	57,1	58,8	67,9	69,6	77,1	83,3	99,2	100
SSI	SSI1	SSI3	SSI6	SSI12	SSI24	SSI1	SSI3	SSI6	SSI12	SSI24
2021-2040	30,4	31,3	32,5	32,5	17,9	0,0	0,0	0,0	0,0	0,0
2041-2060	27,9	26,7	27,1	28,3	22,1	34,6	31,7	30,8	30,0	32,9
2061-2080	62,9	62,1	60,8	58,3	63,3	99,6	99,6	99,6	100	100
2081-2100	68,8	70,4	70,4	70,0	78,3	100	100	100	100	100

While towards the end of the century drought will become increasingly severe and/or widespread, by contrast, for the beginning of the century (period 2021-2040), the percentages of dry years will be relatively very low compared with wet years. On average, they would range between 29.1% under SSP 126 and 5.8% under SSP 585 at the Kolda station, and 27.3% under SSP 126 and 4.9% under SSP 585 at the Wassadou station. For SPI, values ranged from 47.5% under SSP 126 and 13.6% under SSP 585 at the Kolda station, to 46.7% under SSP 126 and 12.7% under SSP 585 at the Wassadou station. Finally, for SSI, the percentages of dry years would be 37.3% under SSP 126 and 0% under SSP 585 at the Kolda station, and 28.9% under SSP 126 and 0% under SSP 585 at the Wassadou station.

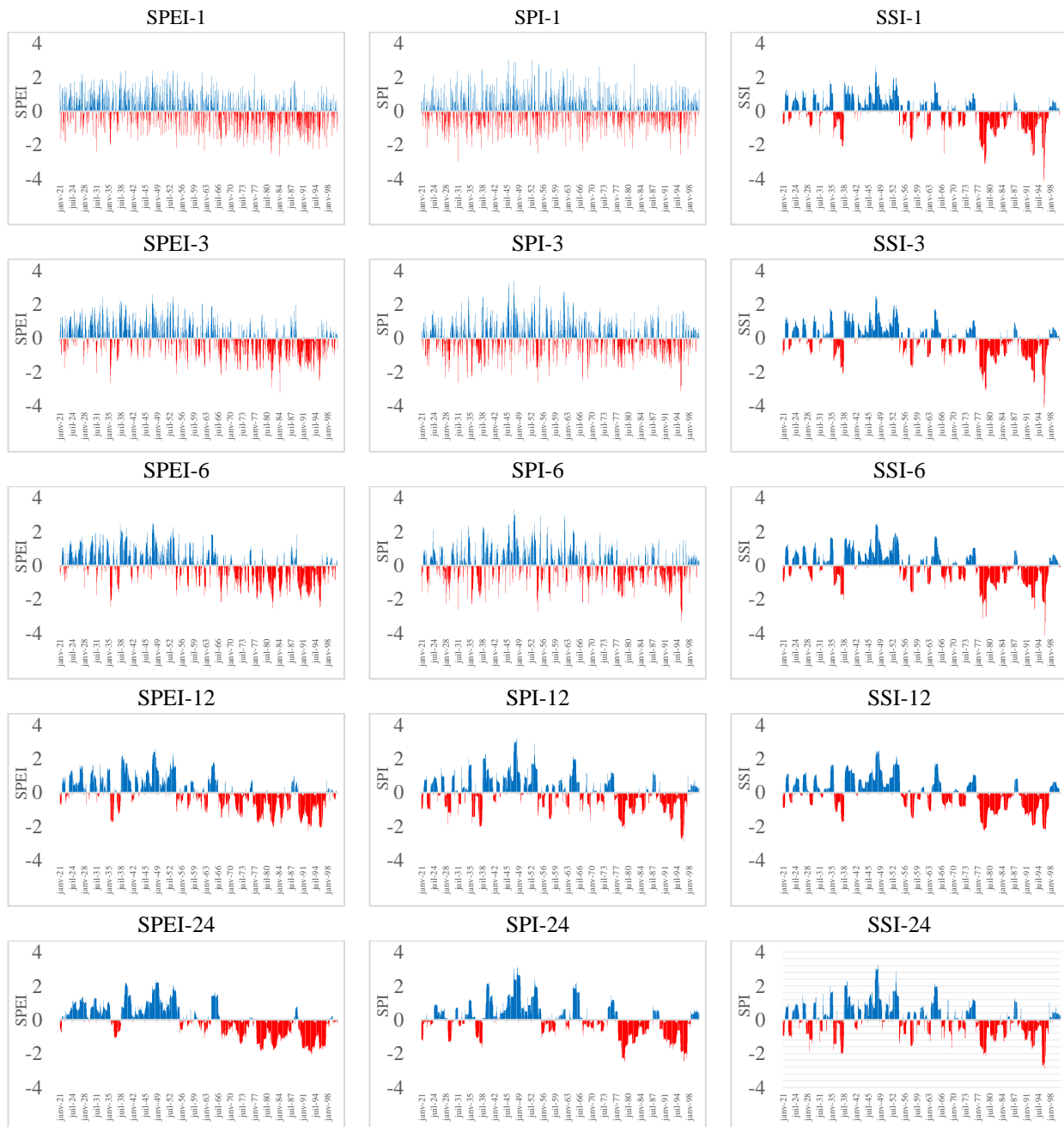


Figure 3. Temporal evolution of SPI, SPEI and SSI values at different time scales over the period 2021-2100 under the SSP 126 scenario in the Casamance basin at Kolda.

The drought in the basins continues to increase over the years in terms of the differences in the SPEI, Spi and SSI indices. In the Casamance basin at the Kolda station, the percentage of dry years in

the SPEI 12 has risen from 28.3% under SSP 126 and 0% under SSP 585 over the period 2021-2040 to 79.2% under SSP 126 and 100% under SSP 585 over the period 2081-2100. In the Kayanga basin at the Wassadou station, the percentage of dry years in SPEI 3 has also risen from 30% under SSP 126 and 7.1% under SSP 585 over the period 2021-2040 to 72.5% under SSP 126 and 92.1% under SSP 585 over the period 2081-2100. The SPEI values are expected to be lower in regions where the temperature would increase more and higher in regions where the temperature is likely to increase less (Montes-Vega et al., 2023). In addition, a significant increase in temperature and a decrease in SPEI were observed under both SSPs in the basins (Figure 4).

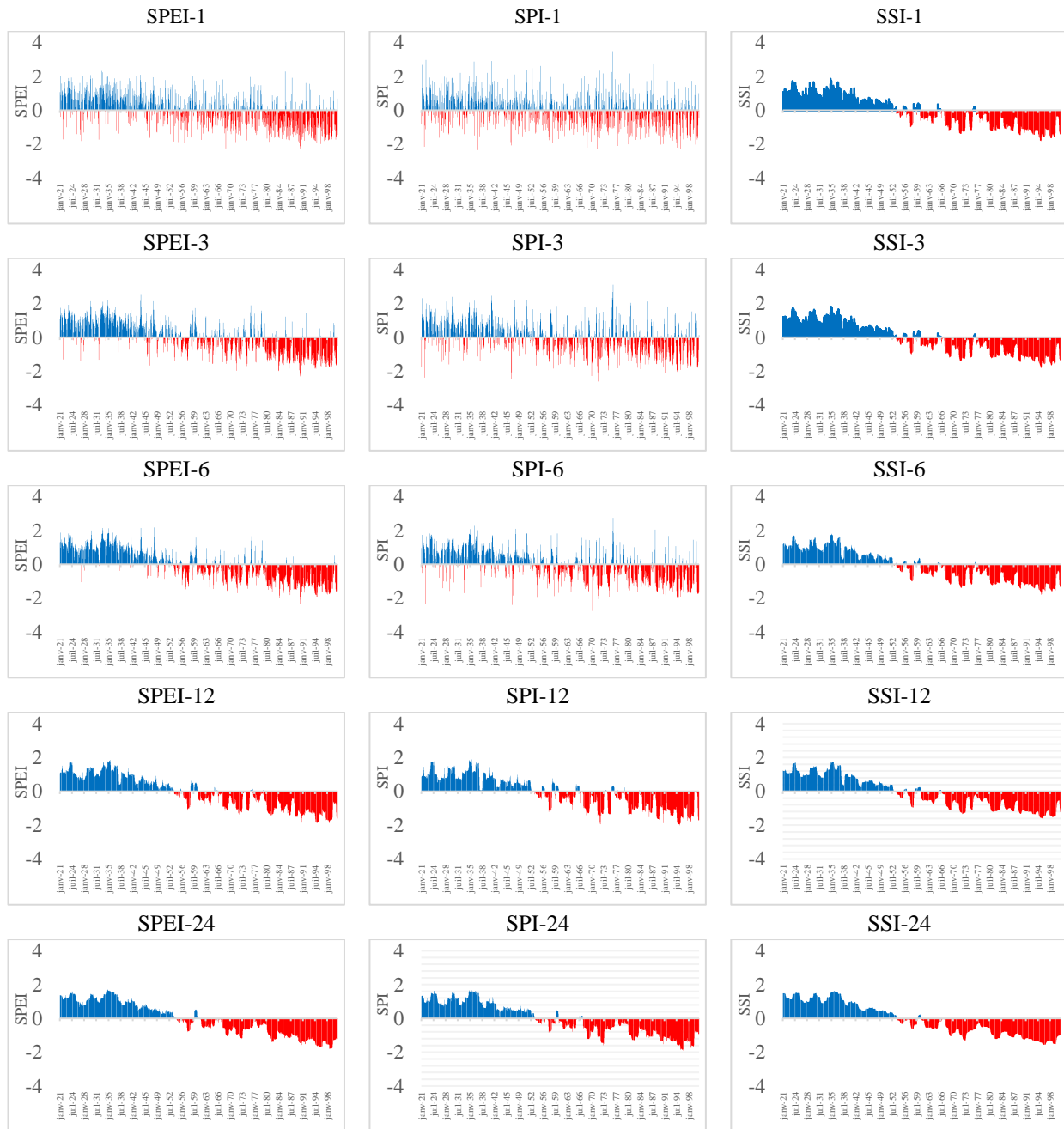


Figure 4. Temporal evolution of SPI, SPEI and SSI values at different time scales over the period 2021-2100 under the SSP 585 scenario in the Casamance basin at Kolda.

The change over time in precipitation, temperature and the SPEI, SPI and SSI indices for SSP 126 was found to follow the same pattern as for SSP 585. The subtle differences were a sharper increase in temperature and a slight increase in precipitation in the latter part of the century for the highest scenario, SSP 585. As a result, the changes in the SPEI, SPI and SSI were not very different between the two scenarios because the impact of a large increase in temperature could be offset by an increase in precipitation (**Figure 4**).

Table 3 gives the Man Kendall trends as well as the Sen slope values of SPEI, SPI and SSI at different time scales over the period 2021-2100 in the Casamance basin at the Kolda station and the Kayanga basin at the Wassadou station. The results of the Man Kendall test analysis reveal that the null hypothesis is rejected for almost all SPEI, SPI and SSI time series (with the exception of SPI1 at Kolda; SPI1 and SPI3 at Wassadou), indicating the existence of a statistically significant trend (p -value < 0.05) at the 95% confidence level.

The Kendall Tau values therefore reflect a statistically significant downward trend in the indices, and thus an increase in the severity of the drought at all time scales in the basins. For the SPEI, Kendall's Tau values vary between -0.439 and -0.192 under SSP 126, and between -0.804 and -0.414 under SSP 585 over the period 2081-2100 at the Kolda station, whereas for Wassadou, they vary between -0.414 and -0.203 under SSP 126, and between -0.806-0.433 under SSP 585. The same applies to the SPI and SSI indices in both basins (**Figure 5**).

The downward trend is more significant under SSP 585 for the SPEI, SPI and SSI. For the SPEI, at the Kolda station, Kendall's tau is -0.192, -0.268, -0.314, -0.358 and -0.439 respectively for SPEI 1, SPEI 3, SPEI 6, SPEI 12 and SPEI 24 under SSP 126, and -0.414, -0.545, -0.641, -0.750 and -0.804 respectively for SPEI 1, SPEI 3, SPEI 6, SPEI 12 and SPEI 24 under SSP 585. It is -0.020, -0.044, -0.087, -0.143 and -0.202 respectively for SPI 1, SPI 3, SPI 6, SPI 12 and SPI 24 under SSP 126, and -0.281, -0.282, -0.280, -0.286 and -0.326 respectively for SPI 1, SPI 3, SPI 6, SPI 12 and SPI 24 under SSP 585. For the SSI, Kendall's tau, always negative, is more significant than for the SPEI and SPI. It is -0.211, -0.313, -0.466, -0.695 and -0.771 respectively for SSI 1, SSI 3, SSI 6, SSI 12 and SSI 24 under SSP 126, and -0.763, -0.766, -0.771, -0.786 and -0.828 respectively for SSI 1, SSI 3, SSI 6, SSI 12 and SSI 24 under SSP 585. The observation remains the same for the Kayanga basin at Wassadou. Trends in hydrological drought are therefore more pronounced than those in meteorological drought, implying that other factors influence the development of hydrological drought ([Bevacqua et al., 2021](#), [Fowé et al., 2023](#)).

Sen's slope estimator revealed the magnitude of the slopes in the SPEI, SPI and SSI time series. Sen's slope analysis shows a decreasing trend for all time series SPEI, SPI and SSI. Moreover, the highest and lowest slope amplitudes were observed for SSI and SPEI respectively (**Figure 6**). According to the trend statistics, meteorological drought (for SPEI and SPI) and hydrological drought showed a significant downward trend over the period 2021-2100 in the Casamance basin at the Kolda station and the Kayanga basin at the Wassadou station. A negative value of Sen's slope translates into an increase in the severity of the drought and a move towards drier conditions.

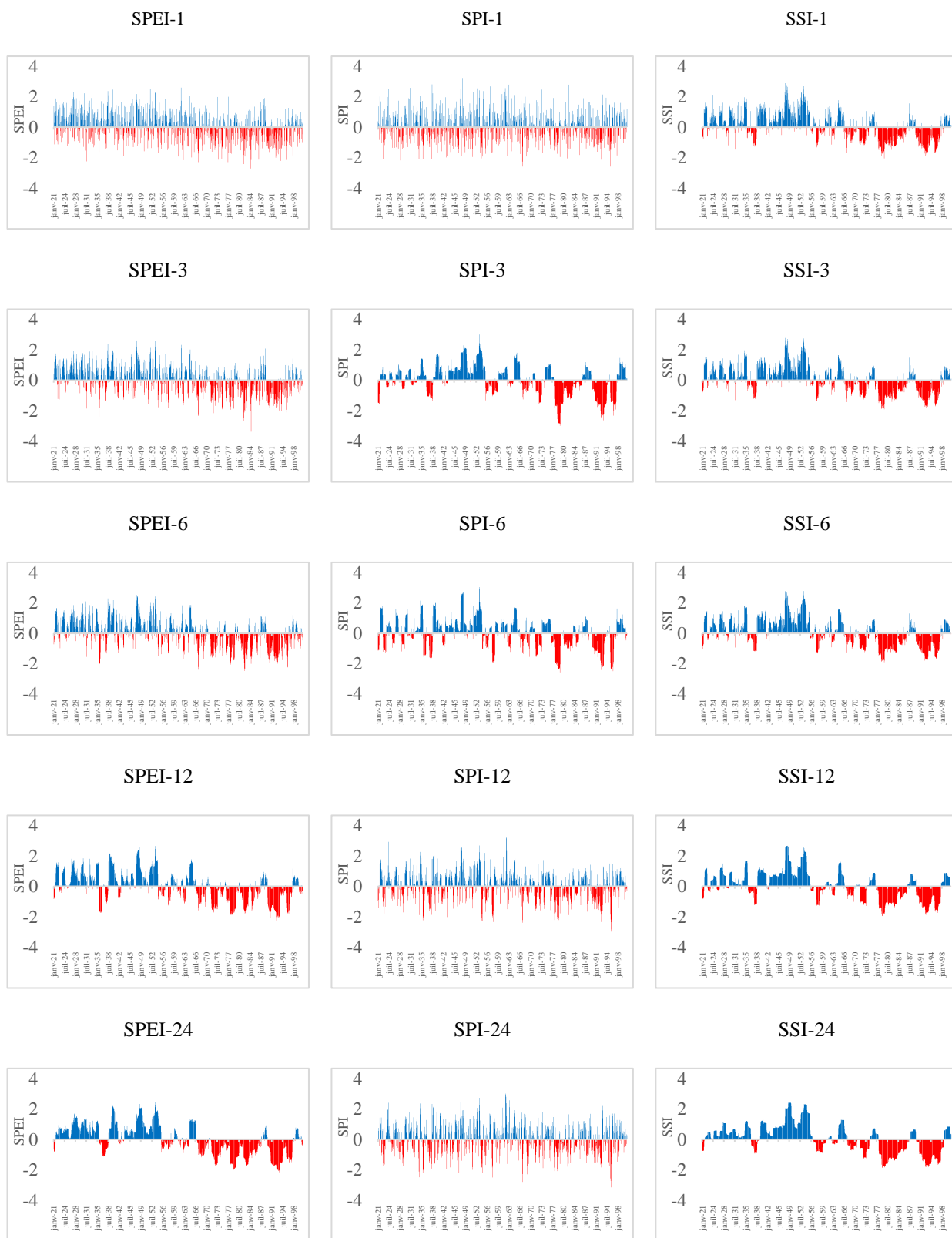


Figure 7. Temporal evolution of SPI, SPEI and SSI values at different time scales over the period 2021-2100 under the SSP 126 scenario in the Kayanga basin at Wassadou

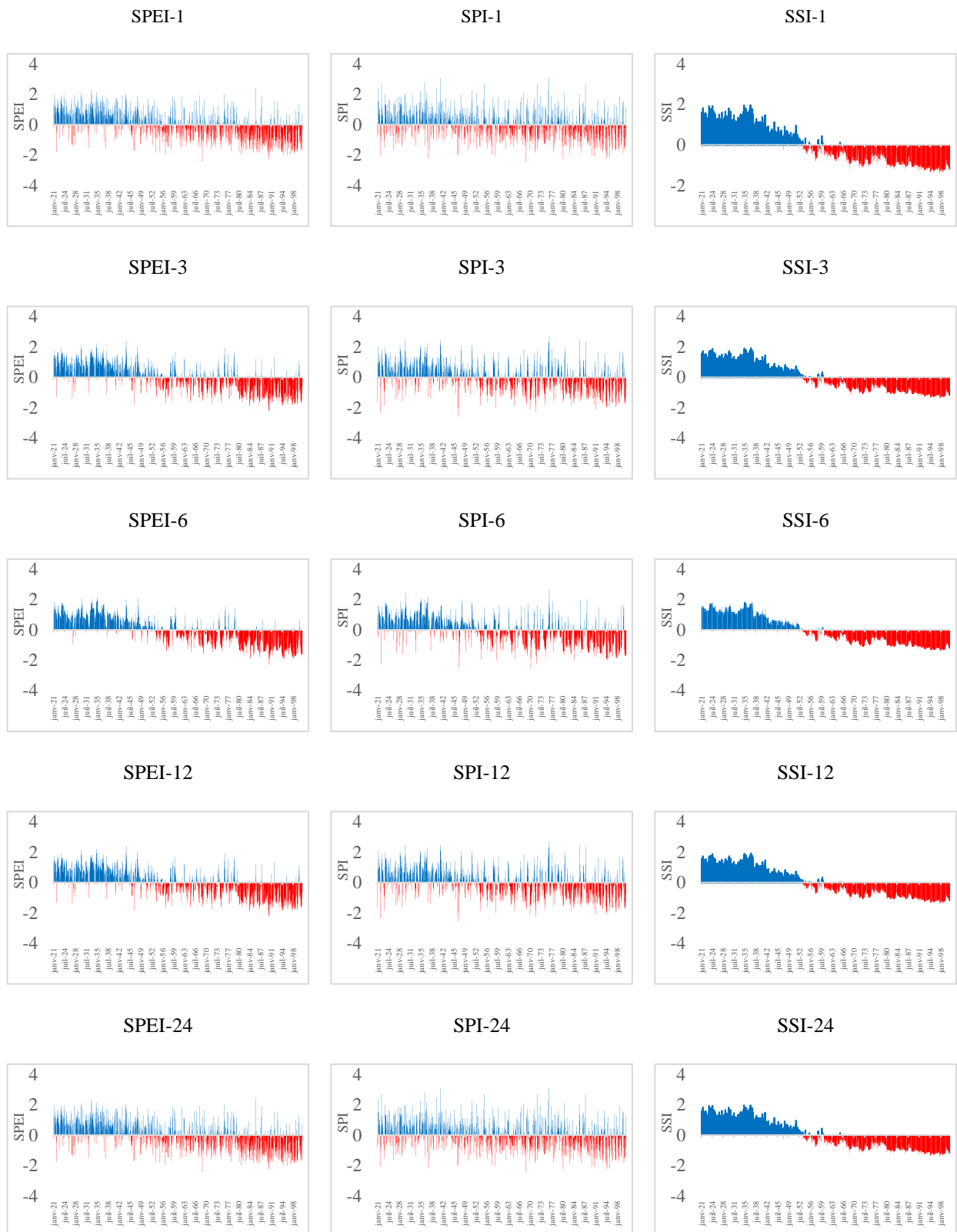


Figure 8. Temporal evolution of SPI, SPEI and SSI values at different time scales over the period 2021-2100 under the SSP 585 scenario in the Kayanga basin at Wassadou.

Table 2. Man Kendall test on the SPEI, SPI and SSI indices by scenario over the period 2021-2100 in the Casamance basin in Kolda and the Kayanga basin in Wassadou

KOLDA	SSP 126					SSP 585				
SPEI	SPEI 1	SPEI 3	SPEI 6	SPEI1 2	SPEI2 4	SPEI 1	SPEI 3	SPEI 6	SPEI1 2	SPEI2 4
Kendall Tau	-0,192	-0,268	-0,314	-0,358	-0,439	-0,414	-0,545	-0,641	-0,750	-0,804
p-value	< 0,0001	< 0,0001	< 0,0001	< 0,0001	< 0,0001	< 0,0001	< 0,0001	< 0,0001	< 0,0001	< 0,0001
Sen slope	-0,001	-0,001	-0,002	-0,002	-0,002	-0,002	-0,003	-0,003	-0,003	-0,003
SPI	SPI1	SPI3	SPI6	SPI12	SPI24	SPI1	SPI3	SPI6	SPI12	SPI24
Kendall Tau	-0,020	-0,044	-0,087	-0,143	-0,202	-0,281	-0,282	-0,280	-0,286	-0,326
p-value	0,328	0,036	< 0,0001	< 0,0001	< 0,0001	< 0,0001	< 0,0001	< 0,0001	< 0,0001	< 0,0001
Sen slope	-0,00005	-0,0002	-0,0004	-0,0007	-0,001	-0,001	-0,001	-0,001	-0,001	-0,002
SSI	SSI1	SSI3	SSI6	SSI12	SSI24	SSI1	SSI3	SSI6	SSI12	SSI24
Kendall Tau	-0,211	-0,313	-0,466	-0,695	-0,771	-0,763	-0,766	-0,771	-0,786	-0,828
p-value	< 0,0001	< 0,0001	< 0,0001	< 0,0001	< 0,0001	< 0,0001	< 0,0001	< 0,0001	< 0,0001	< 0,0001
Sen slope	-0,001	-0,002	-0,002	-0,003	-0,003	-0,003	-0,003	-0,003	-0,003	-0,003
WASSADOU	SSP 126					SSP 585				
SPEI	SPEI1	SPEI3	SPEI6	SPEI12	SPEI24	SPEI1	SPI3	SPI6	SPI12	SPI24
Kendall Tau	-0,203	-0,278	-0,308	-0,338	-0,414	-0,433	-0,560	-0,651	-0,749	-0,806
p-value	< 0,0001	< 0,0001	< 0,0001	< 0,0001	< 0,0001	< 0,0001	< 0,0001	< 0,0001	< 0,0001	< 0,0001
Sen slope	-0,001	-0,001	-0,002	-0,002	-0,002	-0,002	-0,003	-0,003	-0,003	-0,003
SPI	SPI1	SPI3	SPI6	SPI12	SPI24	SPI1	SPI3	SPI6	SPI12	SPI24
Kendall Tau	-0,013	-0,033	-0,068	-0,109	-0,157	-0,214	-0,313	-0,461	-0,689	-0,770
p-value	0,540	0,114	0,001	< 0,0001	< 0,0001	< 0,0001	< 0,0001	< 0,0001	< 0,0001	< 0,0001
Sen slope	-0,0001	-0,0002	-0,0004	-0,001	-0,001	-0,001	-0,002	-0,002	-0,003	-0,003
SSI	SSI1	SSI3	SSI6	SSI12	SSI24	SSI1	SSI3	SSI6	SSI12	SSI24
Kendall Tau	-0,203	-0,210	-0,206	-0,204	-0,238	-0,761	-0,770	-0,774	-0,786	-0,831
p-value	< 0,0001	< 0,0001	< 0,0001	< 0,0001	< 0,0001	< 0,0001	< 0,0001	< 0,0001	< 0,0001	< 0,0001
Sen slope	-0,001	-0,001	-0,001	-0,001	-0,001	-0,003	-0,003	-0,003	-0,003	-0,003

3.3 Drought classification

Table 4 shows the frequency of drought classification based on the three drought indices at different time scales in the Casamance basin at the Kolda station and the Kayanga basin at the Wassadou station. It can be noted that the frequency of drought episodes in a given class varies with the time scale. By scenario, drought occurrences are more important under SSP 585, while by drought index categories, they are more important on the SPEI, could approach or exceed 50%. According to the results, the extreme and severe categories were the least frequently observed (frequency less than 7.0%). For extreme droughts, the maximum frequency observed at the Kolda station on the different time scales was 1.7, 2 and 3.8% respectively for SPEI, SPI and SSI under SSP 126, and 0.3, 1.3 and 0% respectively for SPEI, SPI and SSI. For the Wassadou station, the maximum frequency of extreme droughts on the different time scales is 1.7, 3.4 and 0.1% respectively for SPEI, SPI and SSI under SSP 126, and 0.5, 1.1 and 0% respectively for SPEI, SPI and SSI.

Overall, the projected data predict more frequent risks of mild drought. These light drought occurrence frequencies are generally greater than or equal to 30% under all scenarios (except for SPEI 3 and SPEI 24, SPI 24, SSI 6, SSI 12 and SSI 24 under SSP 585 at the Kolda station). The highest frequency of occurrence of light drought varies from 30.3 to 34.0% for the SPEI, from 33.1 to 35.4% for the SPI and from 32.1 to 39.2% for the SSI under SSP 126 at the Kolda station. Under SSP 585, it varies from 24.0 to 33.2% for the SPEI, from 28.9 to 35.0% for the SPI and from 22.8 to 31.7% for the SSI. Occurrence trends at the Wassadou station are fairly similar to those at the Kolda station. At Wassadou, the frequency of occurrence of mild drought varies from 32 to 32.9% for the SPEI, from 29.8 to 36.1%

for the SPI and from 28.1 to 32.4% for the SSI under SSP 126, and from 30.4 to 35.1% for the SPEI, from 31.4 to 36.6% for the SPI and from 36.8 to 38.0% for the SSI under SSP 585.

Table 3. Drought classification frequency (%), with SPI, SPEI and SSI indices over the 2021-2100 period in the Casamance basin in Kolda and the Kayanga basin in Wassadou

KOLDA	SSP 126					SSP 585				
SPEI	SPEI 1	SPEI 3	SPEI 6	SPEI12	SPEI24	SPEI 1	SPEI 3	SPEI 6	SPEI12	SPEI24
Extremely dry	1,7	1,5	1,7	1,3	0,2	0,3	0,3	0,2	0,0	0,0
Severely dry	4,5	4,9	6,5	7,0	9,5	6,8	6,5	5,7	4,8	5,0
Moderately dry	11,9	11,9	10,3	10,1	8,5	12,5	14,6	17,2	20,0	17,8
Slightly damp	32,8	34,0	33,5	32,4	30,3	33,2	29,6	30,2	29,4	24,0
No drought	49,4	49,7	49,2	48,2	47,7	48,3	46,4	46,3	46,6	43,6
SPI	SPI1	SPI3	SPI6	SPI12	SPI24	SPI1	SPI3	SPI6	SPI12	SPI24
Extremely dry	1,4	1,7	2,0	1,6	1,8	1,3	0,8	0,7	0,1	0,0
Severely dry	3,4	4,2	5,1	5,0	3,5	4,1	5,1	5,7	5,4	4,1
Moderately dry	9,5	8,8	7,5	8,1	11,3	10,0	10,7	13,6	17,7	17,6
Slightly damp	33,1	35,4	33,9	35,3	35,4	35,0	33,6	34,1	32,5	28,9
No drought	49,0	50,9	49,9	50,0	50,3	48,2	47,8	48,2	46,1	44,1
SSI	SSI1	SSI3	SSI6	SSI12	SSI24	SSI1	SSI3	SSI6	SSI12	SSI24
Extremely dry	3,8	3,2	2,8	2,3	1,1	0,0	0,0	0,0	0,0	0,0
Severely dry	3,8	4,2	4,6	4,5	5,3	3,1	2,9	2,3	2,0	2,2
Moderately dry	7,8	9,1	10,0	10,9	10,4	21,4	21,8	22,4	22,7	19,3
Slightly damp	39,2	37,7	35,4	32,1	35,0	31,7	30,5	29,8	27,6	22,8
No drought	51,8	51,1	50,1	48,3	49,6	45,6	45,2	45,0	44,3	42,3
WASSADOU	SSP 126					SSP 585				
SPEI	SPEI1	SPEI3	SPEI6	SPEI12	SPEI24	SPEI1	SPEI3	SPEI6	SPEI12	SPEI24
Extremely dry	1,7	1,7	1,5	0,8	1,0	0,5	0,3	0,1	0,0	0,0
Severely dry	5,1	4,9	6,6	9,1	8,5	6,7	6,3	5,9	4,6	5,2
Moderately dry	11,5	11,6	10,6	8,3	9,5	13,2	15,1	16,3	19,3	15,8
Slightly damp	32,8	32,9	32,2	32,0	32,9	31,9	31,4	30,9	30,4	35,1
No drought	49,0	49,0	49,2	49,8	48,0	47,7	47,0	46,8	45,7	43,9
SPI	SPI1	SPI3	SPI6	SPI12	SPI24	SPI1	SPI3	SPI6	SPI12	SPI24
Extremely dry	1,3	1,9	2,8	3,4	2,9	1,1	0,8	0,7	0,0	0,0
Severely dry	3,1	5,4	4,2	3,9	5,8	4,2	4,6	5,8	6,1	4,1
Moderately dry	9,8	8,0	9,4	8,3	7,9	9,9	11,8	13,3	16,3	14,9
Slightly damp	36,1	34,0	31,7	29,8	31,9	35,8	35,0	32,1	31,4	36,6
No drought	49,7	50,7	52,0	54,6	51,5	49,0	47,8	48,0	46,3	44,5
SSI	SSI1	SSI3	SSI6	SSI12	SSI24	SSI1	SSI3	SSI6	SSI12	SSI24
Extremely dry	0,1	0,0	0,0	0,0	0,0	0,0	0,0	0,0	0,0	0,0
Severely dry	3,1	3,4	3,5	4,1	6,1	0,0	0,0	0,0	0,0	0,0
Moderately dry	11,9	12,3	13,6	15,1	9,6	19,7	20,4	20,8	20,5	20,0
Slightly damp	32,4	31,9	30,5	28,1	29,7	38,9	37,4	36,8	37,0	38,2
No drought	52,5	52,4	52,3	52,7	54,6	41,5	42,2	42,4	42,5	41,8

The values in red represent the maximum frequencies of the different drought classes for the drought indices at different time scales.

For mild drought, the maximum frequency is generally observed over a time scale of 3 months for SPEI and SPI, and 1 month for SSI. For moderate drought, maximum frequency is observed over time scales of 1, 12 and 24 months under both scenarios in Kolda with values of 11.9, 11.3 and 10.9% respectively for SPI, SPEI and SSI under SSP 126, and 20.0, 17.7 and 22.7% respectively for SPI, SPEI and SSI under SSP 585. There is a similarity between SPEI, SPI and SSI for the frequencies of the different drought classes on the time scales. The SPEI, SPI and SSI values at different time scales showed that light and moderate droughts dominated in the Casamance basins at the Kolda station and the Kayanga at the Wassadou station during the period 2021-2100.

4.4 Analysis of the meteorological and hydrological characteristics of the drought

Drought events are taken into account for drought index values below -1 in this study. Drought events and drought characteristics in the Casamance basin at the Kolda station and the Kayanga basin at the Wassadou station were identified and extracted by decade using Run theory and are presented in **Figures 7, 8, 9 and 10**. The longer size of the box or the longer range of the moustache means that there is a wide range of changes in the SPEI, SPI and SSI indices for different periods, while the shorter size or a shorter moustache shows a closeness in the values of these parameters. It can be seen that while there is no significant change in the indices in either basin under SSP 126 over the 2021-2100 period, under SSP 585 there is a significant change in the indices in both basins over the 2021-2100 period. While the indices are expected to be mainly constant and the size of the boxes to decrease slightly over the last fifty years of the century under SSP 126, they increase sharply over the last fifty years of the century under SSP 585. Box height was found to increase progressively under both SSPs, but much more under SSP 585 than SSP 126, in both basins (**Figures 7, 8, 9 and 10**). This indicates greater homogeneity in the spatial distribution of precipitation in the two basins over the period studied.

At the Kolda station, the most important drought events under the SSP 126 scenario are SSI 24 with a drought duration of 72 months from 2081 to 2100 and a severity of 111, SPEI 24 with a duration of 71 months from 2081 to 2100 and a severity of 115, and SPI 24, with a duration of 66 months between 2081 and 2100 and a severity of 103. Under the SSP 585 scenario, these are SPEI 24 with a drought duration of 120 months from 2081 to 2100 and a severity of 172, SSI 24 with a duration of 116 months from 2081 to 2100 and a severity of 155, and SPI 24, with a duration of 104 months between 2081 and 2100 and a severity of 147. At the Wassadou station, the trends remain the same, with the SPEI, SPI and SSI indices recording their longest duration on a 24-month scale. Furthermore, the longest (duration) and most severe (severity) droughts are not necessarily the most intense on longer time scales (12 and 24 months). Indeed, at shorter time scales (1, 3, 6 months), drought intensities (in median value) are higher and progressively decrease at longer time scales for all indices, suggesting moderating effects on hydrological cycle components such as soil moisture (1 to 3 months) and surface water resources (6 months).

Changes in precipitation, temperature and runoff would lead to changes in the EPSI, SPI and SSI over time. It was also found that the expected changes in SPEI, SPI and SSI would vary considerably for different periods and scenarios. The average SPEI, SPI and SSI in both basins under both scenarios are expected to decrease over the years, with a much larger decrease towards the end of the century. Although the average SPEI, SPI and SSI have been projected to change less, the height of the box showing the spatial and temporal variability of the indices for different 10-year periods for different scenarios and basins has been projected to vary significantly. The temporal variability of the SPEI, SPI and SSI indices should gradually decrease between the two basins.

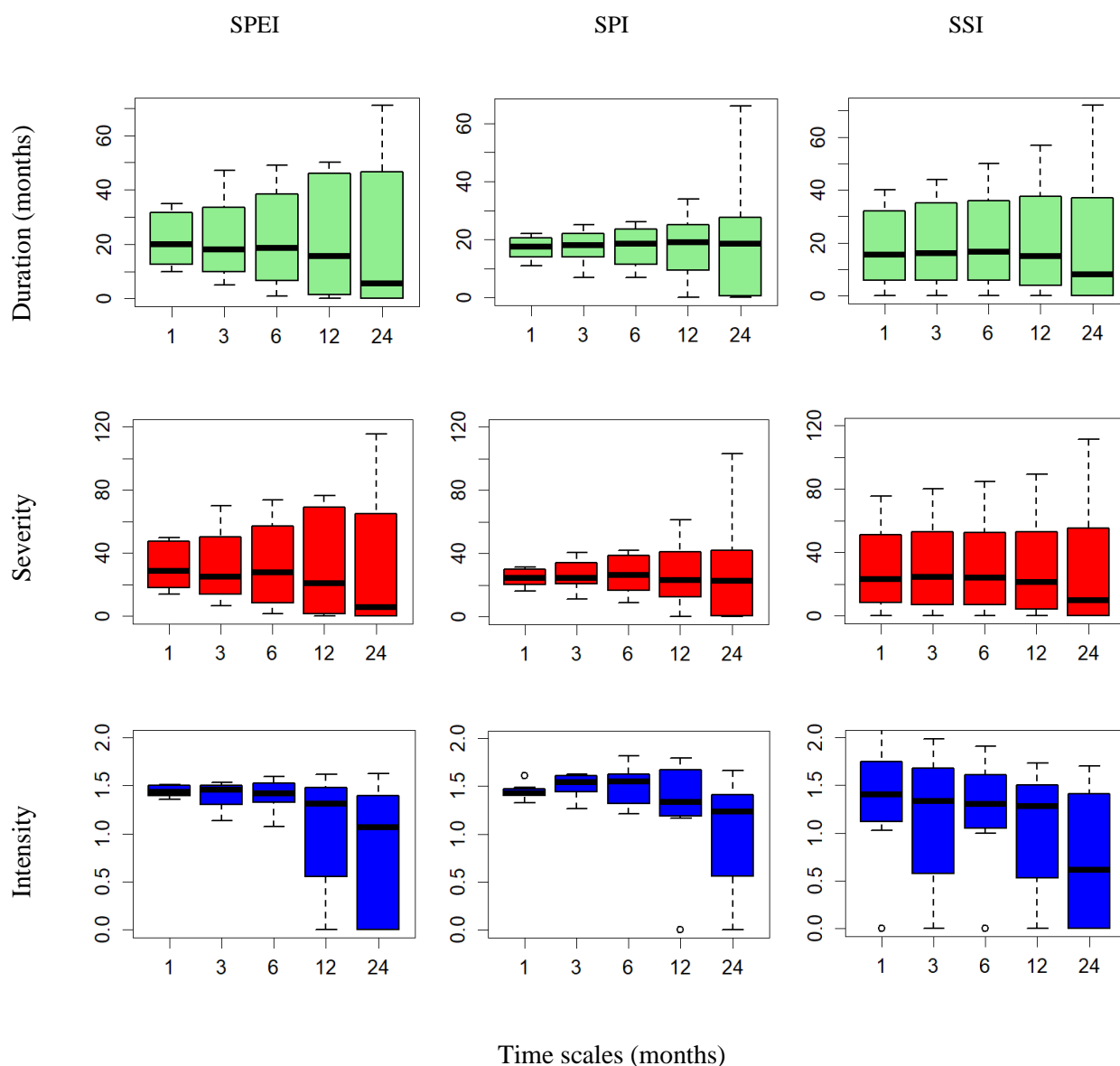


Figure 9. Boxplots showing the meteorological and hydrological characteristics of the drought based on the SPI (green), SPEI (red) and SSI (blue) at different time scales (1, 3, 6, 12 and 24 months) per decade over the period 2021-2100 under the SSP 126 scenario in the Casamance basin in Kolda.

The statistical results of drought characteristics such as duration, severity and intensity based on the SPI, SPEI and SSI are presented in [Table 5](#). It can be observed that drought duration and severity increase with time scales, while the opposite occurs for the number of drought events, which is consistent with previous studies ([Barker et al., 2016](#), [Wu et al., 2018](#), [Abbas et al., 2021](#), [Li et al., 2021](#), [Fowé et al., 2023](#)). For SPEI, the mean value for duration per decade ranged from 21.9 months under SSP 126 to 26.8 months under SSP 585 at the Kolda station, and from 22.2 months under SSP 126 to 26.2 months under SSP 585 at the Wassadou station. For severity, the mean value per dekad is 32 under SSP 126 and 36.2 under SSP 585 at the Kolda station, and 32.6 under SSP 126 and 35.8 under SSP 585 at the Wassadou station. Finally, for intensity, the mean value per dekad ranged from 1.2 under SSP 126 to 0.98 under SSP 585 at the Kolda station, and from 1.18 under SSP 126 to 0.96 under SSP 585 at the Wassadou station ([Table 5](#)).

The shapes of the boxes reflect the distribution of values. An elongated shape indicates a wide distribution of values, while a rounded shape indicates a concentration of values.

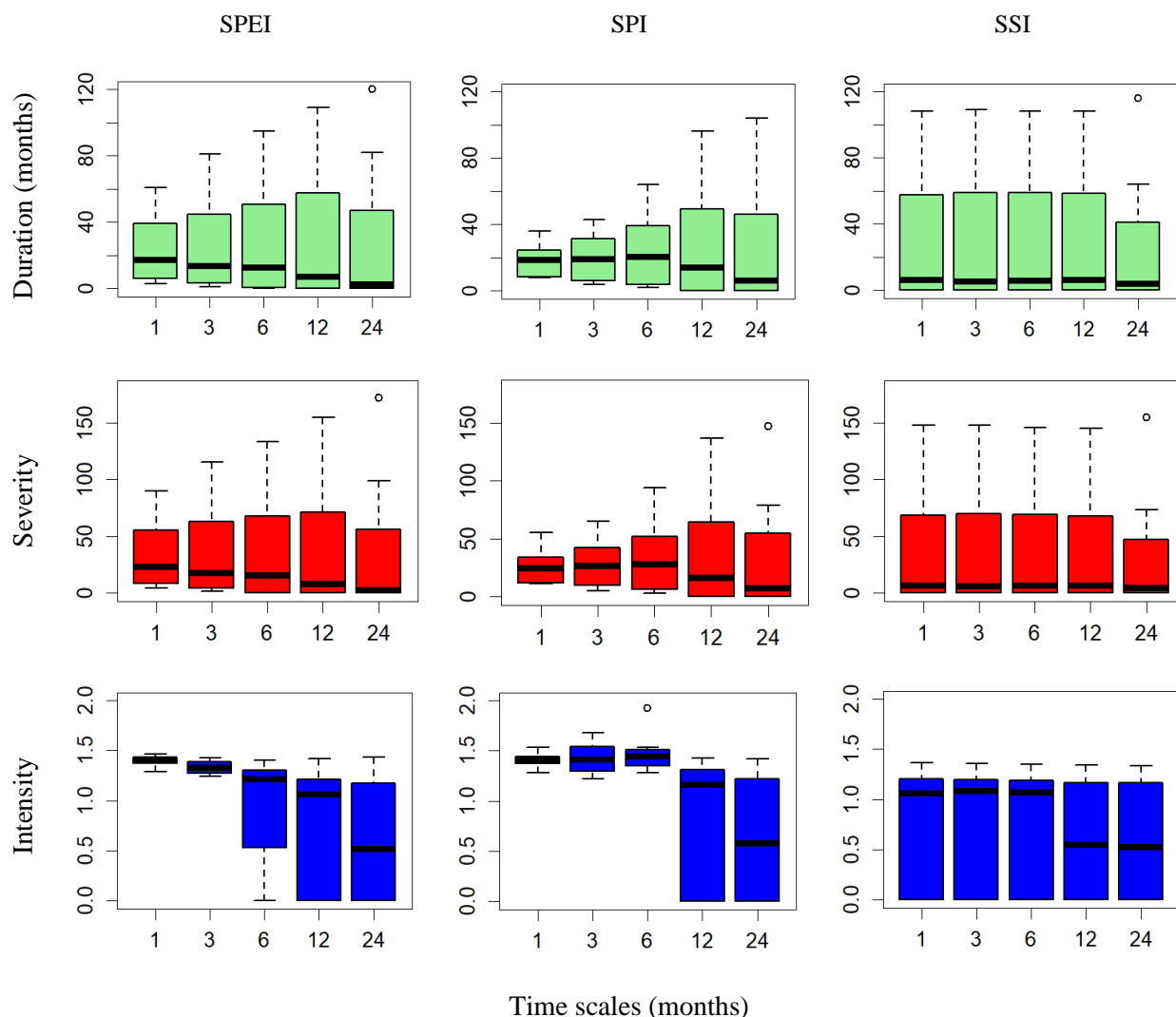


Figure 10. Boxplots showing the meteorological and hydrological characteristics of the drought based on the SPI (green), SPEI (red) and SSI (blue) at different time scales (1, 3, 6, 12 and 24 months) per decade over the period 2021-2100 under the SSP 585 scenario in the Casamance basin at Kolda.

For SPI, the mean value for duration per decade is between 17.9 months under SSP 126 and 23.3 months under SSP 585 at the Kolda station, and 18.7 months under SSP 126 and 22.5 under SSP 585 at the Wassadou station. For severity, the mean value per dekad is 26.8 under SSP 126 and 31.8 under SSP 585 at the Kolda station, and 29 under SSP 126 and 31.4 under SSP 585 at the Wassadou station. Finally, for intensity, the mean value per dekad ranged from 1.34 under SSP 126 to 1.14 under SSP 585 at the Kolda station, and from 1.4 under SSP 126 to 1.14 under SSP 585 at the Wassadou station (**Table 5**). Finally, for SSI, the mean value for duration per decade ranged from 20.1 months under SSP 126 to 28.8 months under SSP 585 at the Kolda station, and from 19.9 months under SSP 126 to 24.3 months under SSP 585 at the Wassadou station. For severity, the mean value per dekad is 30.6 under SSP 126 and 36.0 under SSP 585 at the Kolda station, and 26.6 under SSP 126 and 28.2 under SSP 585 at the Wassadou station. Finally, for intensity, the mean value per dekad ranged from 1.06 under SSP 126 to 0.66 under SSP 585 at the Kolda station, and from 0.9 under SSP 126 to 0.52 under SSP 585 at the Wassadou station (**Table 5**).

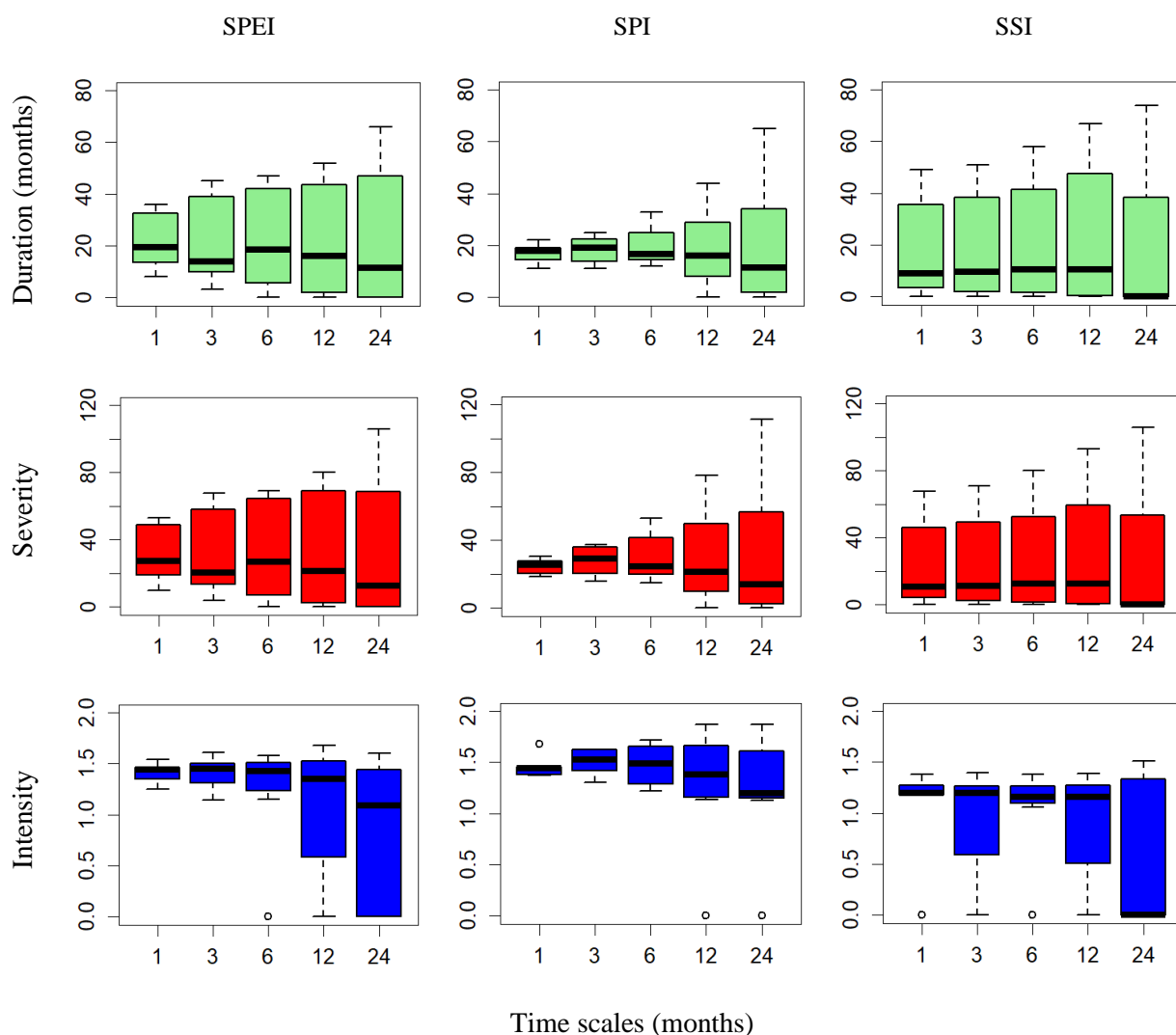


Figure 11. Boxplots showing the meteorological and hydrological characteristics of the drought based on the SPI (green), the SPEI (red) and the SSI (blue) at different time scales (1, 3, 6, 12 and 24 months) per decade over the period 2021-2100 under the SSP 126 scenario in the Kayanga basin at Wassadou.

At shorter time scales (1, 3 and 6 months), the number of meteorological drought events is greater than that of hydrological drought events, indicating that there may be an amount of meteorological drought that does not trigger hydrological drought, probably due to soil surface conditions (Sidibé et al., 2019). The average drought duration and severity of meteorological drought and hydrological drought increased with increasing time scales. Moreover, on both shorter and longer time scales, the average duration of hydrological drought was greater than that of meteorological drought. In terms of drought intensity, meteorological drought was more intense than hydrological drought on shorter time scales (1 month). The characteristics of hydrological droughts are different from those of meteorological droughts.

Table 4. Drought characteristics of the SPI, SPEI and SSI at time scales of 1, 3, 6, 12 and 24 months over the period 2021-2100 in the Casamance basin in Kolda and the Kayanga basin in Wassadou.

KOLDA	SSP 126					SSP 585				
SPEI	SPEI 1	SPEI 3	SPEI 6	SPEI 12	SPEI 24	SPEI 1	SPEI 3	SPEI 6	SPEI 12	SPEI 24
Number of events	175	176	177	175	173	219	238	222	205	188
Average duration/decade	21,9	22	22,1	21,9	21,6	27,4	29,8	27,8	25,6	23,5
Total severity	-257	-260	-261	-254	-251	-290	-313	-300	-286	-266
Average severity/decade	-32	-32	-33	-32	-31	-36	-39	-37	-36	-33
Series intensity	-1,5	-1,5	-1,5	-1,5	-1,5	-1,3	-1,3	-1,4	-1,4	-1,4
Average intensity/decade	-0,8	-1	-1,4	-1,4	-1,4	-0,6	-0,7	-0,9	-1,3	-1,4
SPI	SPI1	SPI3	SPI6	SPI12	SPI24	SPI1	SPI3	SPI6	SPI12	SPI24
Number of events	159	141	140	140	137	208	223	193	160	147
Average duration/decade	19,9	17,6	17,5	17,5	17,1	26	27,9	24,1	20	18,4
Total severity	-234	-215	-214	-211	-197	-270	-298	-270	-226	-208
Average severity/decade	-29	-27	-27	-26	-25	-34	-37	-34	-28	-26
Series intensity	-1,5	-1,5	-1,5	-1,5	-1,4	-1,3	-1,3	-1,4	-1,4	-1,4
Average intensity/decade	-1	-1,3	-1,5	-1,5	-1,4	-0,6	-0,8	-1,5	-1,4	-1,4
SSI	SSI1	SSI3	SSI6	SSI12	SSI24	SSI1	SSI3	SSI6	SSI12	SSI24
Number of events	162	170	167	158	147	206	237	237	237	235
Average duration/decade	20,3	21,3	20,9	19,8	18,4	25,8	29,6	29,6	29,6	29,4
Total severity	-242	-246	-252	-249	-241	-258	-294	-297	-299	-298
Average severity/decade	-30	-31	-31	-31	-30	-32	-37	-37	-37	-37
Series intensity	-1,5	-1,4	-1,5	-1,6	-1,6	-1,3	-1,2	-1,3	-1,3	-1,3
Average intensity/decade	-0,7	-1	-1,2	-1,1	-1,3	-0,6	-0,6	-0,7	-0,7	-0,7
WASSADOU	SSP 126					SSP 585				
SPEI	SPEI1	SPEI3	SPEI6	SPEI12	SPEI24	SPEI1	SPEI3	SPEI6	SPEI12	SPEI24
Number of events	183	175	179	174	175	202	229	214	208	196
Average duration/decade	22,9	21,9	22,4	21,8	21,9	25,3	28,6	26,8	26	24,5
Total severity	-268	-266	-266	-255	-253	-274	-305	-292	-289	-274
Average severity/decade	-33	-33	-33	-32	-32	-34	-38	-37	-36	-34
Series intensity	-1,5	-1,5	-1,5	-1,5	-1,4	-1,4	-1,3	-1,4	-1,4	-1,4
Average intensity/decade	-0,8	-1,1	-1,2	-1,4	-1,4	-0,6	-0,7	-0,8	-1,3	-1,4
SPI	SPI1	SPI3	SPI6	SPI12	SPI24	SPI1	SPI3	SPI6	SPI12	SPI24
Number of events	160	150	157	147	136	182	215	191	165	146
Average duration/decade	20	18,8	19,6	18,4	17	22,8	26,9	23,9	20,6	18,3
Total severity	-257	-239	-239	-223	-196	-246	-292	-268	-232	-206
Average severity/decade	-32	-30	-30	-28	-25	-31	-37	-34	-29	-26
Series intensity	-1,6	-1,6	-1,5	-1,5	-1,4	-1,3	-1,4	-1,4	-1,4	-1,4
Average intensity/decade	-1,2	-1,3	-1,5	-1,5	-1,5	-0,6	-0,8	-1,5	-1,4	-1,4
SSI	SSI1	SSI3	SSI6	SSI12	SSI24	SSI1	SSI3	SSI6	SSI12	SSI24
Number of events	151	184	165	151	145	192	197	200	196	189

Average duration/decade	18,9	23	20,6	18,9	18,1	24	24,6	25	24,5	23,6
Total severity	-213	-238	-213	-197	-189	-227	-232	-232	-225	-216
Average severity/decade	-27	-30	-27	-25	-24	-28	-29	-29	-28	-27
Series intensity	-1,4	-1,3	-1,3	-1,3	-1,3	-1,2	-1,2	-1,2	-1,1	-1,1
Average intensity/decade	-0,5	-0,9	-1,1	-0,9	-1,1	-0,4	-0,4	-0,6	-0,6	-0,6

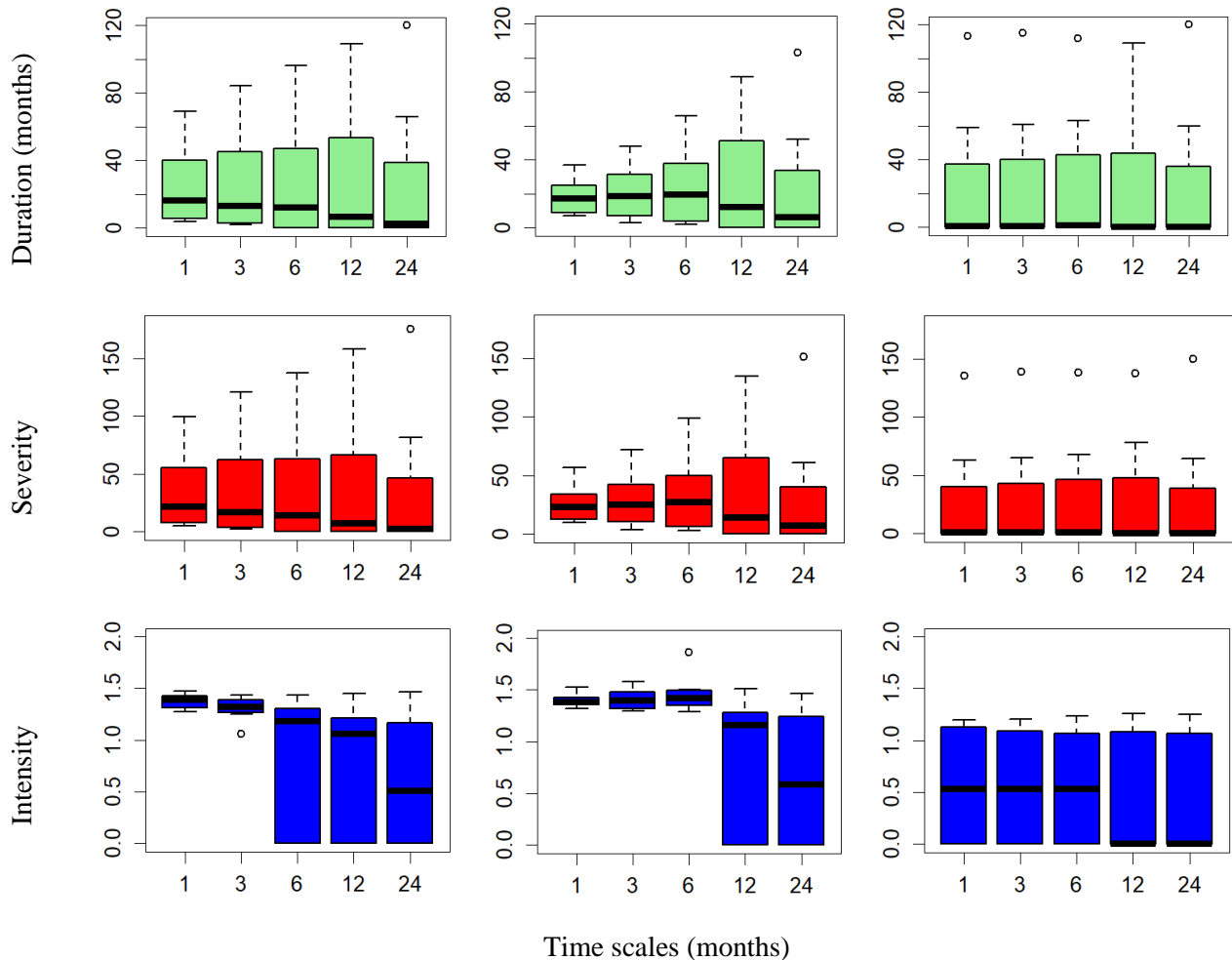


Figure 12. Boxplots showing the meteorological and hydrological characteristics of the drought based on the SPI (green), the SPEI (red) and the SSI (blue) at different time scales (1, 3, 6, 12 and 24 months) per decade over the period 2021-2100 under the SSP 585 scenario in the Kayanga basin at Wassadou.

4.5 Propagation from meteorological drought to hydrological drought

The Pearson correlation coefficients between the SPEI-SSI and SPI-SSI drought indices at different time scales (1, 3, 6, 12 and 24 months) over the period 2021-2100 in the Casamance river basins at the Kolda station and the Kayanga river basin at the Wassadou station are presented in [Table 6](#). Correlation analysis revealed a significant positive linear relationship (r : 0.061 to 0.988, p -values < 0.05) between meteorological and hydrological drought indices at all time scales. This indicates that the meteorological drought in the Casamance basins at the Kolda station and the Kayanga at the Wassadou station is probably the cause of the hydrological drought in the same area. The SPEI, SPI and SSI indices (on the various scales) were found to be negatively correlated with temperature and positively correlated with rainfall. The results indicate that temperature would play a vital role in increasing

droughts under both scenarios. Consequently, precipitation and temperature would play a crucial role in defining the severity of drought at the end of the century under both scenarios.

The correlation between the meteorological and hydrological drought indices was significant for both basins and both scenarios. Under SSP 126, the correlation reached 24-month values of 0.888 between SPEI-SSI and SPI-SSI, 0.887 between SPI-SSI and SPI-SSI in Kolda, and 0.760 between SPEI-SSI and SPI-SSI, and 0.830 between SPI-SSI and SPI-SSI in Wassadou. Under SSP 585, the correlation at the 24-month scale reached values of 0.988 between SPEI-SSI and SPI-SSI, 0.986 between SPI-SSI and SPI-SSI in Kolda, and 0.964 between SPEI-SSI and SPI-SSI, and 0.955 between SPI-SSI and SPI-SSI in Wassadou. It can be seen that the correlation between SPEI-SSI and SPI-SSI increases with the time scale. At the Kolda station, under the SSP 585 scenario, the correlation of SPEI 24 is 0.910 with SSI1, 0.919 with SSI3, 0.934 with SSI6, 0.955 with SSI12 and 0.988 with SSI24, while the correlation of SPI 24 is 0.915 with SSI1, 0.925 with SSI3, 0.938 with SSI6, 0.959 with SSI12 and 0.986 with SSI24.

Table 5. Pearson correlation coefficients between meteorological and hydrological droughts over the period 2021-2100 in the Casamance basin at Kolda and the Kayanga basin at Wassadou

SPEI - SSI Kolda / SSP 126						SPI - SSI Kolda / SSP 126						Corr 1.0 0.5 0.0 -0.5 -1.0
Variables	SSI1	SSI3	SSI6	SSI12	SSI24	Variables	SSI1	SSI3	SSI6	SSI12	SSI24	
SPEI1	0,336	0,269	0,229	0,195	0,205	SPI1	0,248	0,151	0,105	0,061	0,078	
SPEI3	0,506	0,474	0,416	0,352	0,333	SPI3	0,420	0,364	0,277	0,194	0,179	
SPEI6	0,668	0,655	0,631	0,537	0,476	SPI6	0,612	0,583	0,537	0,415	0,346	
SPEI12	0,822	0,839	0,857	0,830	0,686	SPI12	0,842	0,857	0,872	0,812	0,627	
SPEI24	0,718	0,740	0,767	0,816	0,888	SPI24	0,742	0,767	0,798	0,849	0,887	
SPEI - SSI Kolda / SSP 585						SPI - SSI Kolda / SSP 585						
Variables	SSI1	SSI3	SSI6	SSI12	SSI24	Variables	SSI1	SSI3	SSI6	SSI12	SSI24	
SPEI1	0,594	0,572	0,566	0,562	0,562	SPI1	0,317	0,292	0,294	0,289	0,297	
SPEI3	0,768	0,763	0,748	0,740	0,729	SPI3	0,478	0,460	0,449	0,436	0,435	
SPEI6	0,872	0,875	0,875	0,858	0,836	SPI6	0,696	0,693	0,678	0,651	0,628	
SPEI12	0,944	0,953	0,965	0,973	0,942	SPI12	0,942	0,950	0,960	0,959	0,909	
SPEI24	0,910	0,919	0,934	0,955	0,988	SPI24	0,915	0,925	0,938	0,959	0,986	
SPEI - SSI Wassadou / SSP 126						SPI - SSI Wassadou / SSP 126						
Variables	SSI1	SSI3	SSI6	SSI12	SSI24	Variables	SSI1	SSI3	SSI6	SSI12	SSI24	
SPEI1	0,409	0,311	0,262	0,176	0,171	SPI1	0,391	0,231	0,176	0,071	0,045	
SPEI3	0,469	0,494	0,417	0,314	0,282	SPI3	0,435	0,443	0,326	0,193	0,130	
SPEI6	0,593	0,598	0,605	0,479	0,390	SPI6	0,604	0,587	0,587	0,405	0,271	
SPEI12	0,698	0,730	0,744	0,720	0,543	SPI12	0,757	0,790	0,809	0,781	0,514	
SPEI24	0,705	0,737	0,755	0,772	0,760	SPI24	0,761	0,799	0,826	0,852	0,830	
SPEI - SSI Wassadou / SSP 585						SPI - SSI Wassadou / SSP 585						
Variables	SSI1	SSI3	SSI6	SSI12	SSI24	Variables	SSI1	SSI3	SSI6	SSI12	SSI24	
SPEI1	0,628	0,594	0,587	0,570	0,575	SPI1	0,380	0,324	0,318	0,298	0,307	
SPEI3	0,758	0,771	0,750	0,736	0,734	SPI3	0,498	0,494	0,465	0,444	0,445	
SPEI6	0,851	0,854	0,863	0,841	0,829	SPI6	0,668	0,664	0,672	0,636	0,622	
SPEI12	0,930	0,936	0,940	0,937	0,915	SPI12	0,904	0,910	0,915	0,909	0,874	
SPEI24	0,957	0,962	0,967	0,970	0,964	SPI24	0,953	0,959	0,963	0,966	0,955	

Based on the results, the very high correlations between SPEI-SSI (0.830 under SSP 126 and 0.976 under SSP 585 in Kolda) and SPI-SSI (0.812 under SSP 126 and 0.959 under SSP 585 in Kolda) recorded on a 12-month time scale are probably related to the annual hydrological cycle in the study area. This suggests that runoff in the study area is more closely related to meteorological indices on

longer time scales than on shorter ones. According to (Wang et al., 2020), the propagation time from meteorological drought to hydrological drought can be obtained from the maximum correlation coefficients between drought indices at different time scales.

The propagation time from meteorological drought to hydrological drought in these catchments is therefore annual (around 12 or 24 months). In this respect, the development of hydrological drought from meteorological drought takes time in the Casamance catchment at the Kolda station and the Kayanga catchment at the Wassadou station. This may be due to changes in hydrological processes in the catchment as a result of climatic and environmental changes (Descroix et al., 2018, Yonaba et al., 2023, Gbohoui et al., 2021, Fowé et al., 2023).

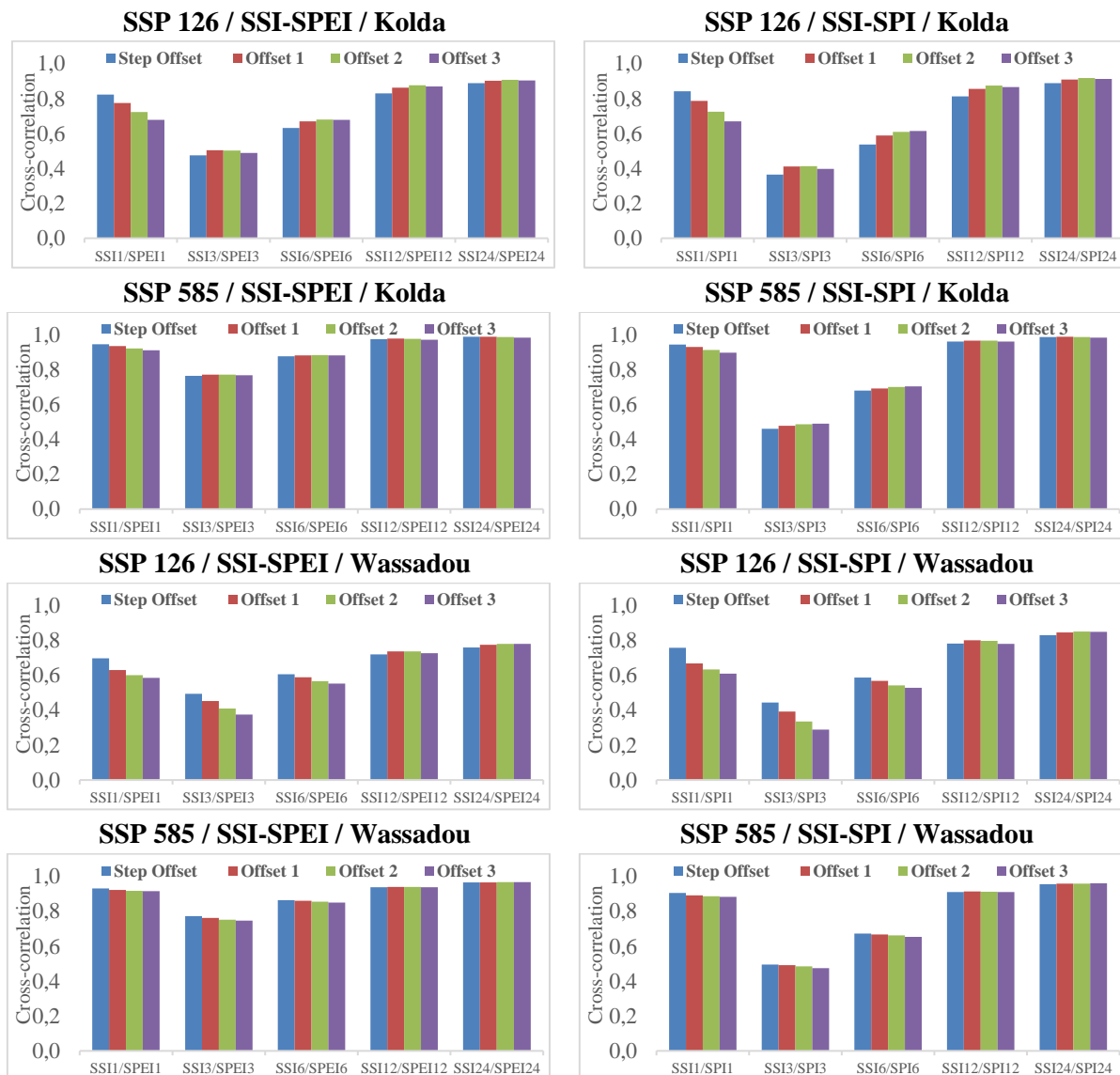


Figure 13. Cross-correlation between meteorological and hydrological droughts on different time scales (SSI-SPEI and SSI-SPI) over the period 2021-2100 in the Casamance basin in Kolda and the Kayanga basin in Wassadou.

The cross-correlation between SSI-SPEI and SSI-SPI at different lags is shown in Figure 10. According to the results, in the Casamance basin at the Kolda station and in the Kayanga basin at the Wassadou station, the highest cross-correlations between SPEI-SSI and SPI-SSI are observed on a time scale of 12 and 24 months and are more significant for SPEI-SSI than for SPI-SSI, albeit slightly. The

cross-correlations decrease with time lag on all time scales, on both relationships (SPEI-SSI and SPI-SSI) and on both scenarios studied in both basins. However, this decrease is more apparent for the 1, 3 and 6-month time scales. Very high correlation coefficients between SPI and SSI, with values greater than 0.8 (0.856 under SSP 126 and 0.965 under SSP 585 in Kolda; 0.800 under SSP 126 and 0.913 under SSP 585 in Wassadou) at lag 1, were observed respectively on the 12-month time scales. This means that the hydrological drought in the study area responds to the meteorological drought at lag 1. Overall, there is no significant lag effect between the meteorological and hydrological droughts in these two basins ([Figure 14](#)). This means that meteorological drought in the catchment areas immediately affects surface water resources.

5. Discussions

Accurate knowledge of climate change is important for dealing with the likelihood of natural disasters. We show the individual changes in precipitation due to global warming under the SSP 126 and SSP 585 scenarios on the basis of the CMIP6 analysis in terms of precipitation and temperature in the Casamance basins at the Kolda station and the Kayanga at the Wassadou station. By the end of the 21st century, the greatest decrease in rainfall is projected in the Casamance basins at the Kolda station and the Kayanga at the Wassadou station, while temperatures will rise sharply. This trend of decreasing annual rainfall is highly variable, but the region in which the basins are located and the evidence of this rainfall variability are consistent with the projections of the Intergovernmental Panel on Climate Change ([IPCC, 2019](#)). These changes in precipitation patterns are driven by changes in continental and sea surface temperatures as well as variations in wind patterns and ocean currents ([IPCC, 2007](#)). The variability was consistent with other research, which has predicted decreases in rainfall over West Africa.

The changes in drought detected using the SPEI show a greater increase in terms of intensity and extent, which corresponds to the sensitivity of the index to changes in evaporation demand caused by the increase in temperature. Temperature increases affect the severity of droughts by increasing evaporation losses, amplifying soil moisture and runoff deficits, despite smaller variations in rainfall. The Casamance basin at the Kolda station and the Kayanga basin at the Wassadou station would experience statistically significant changes corresponding to an increase in the percentage of dry years, with the highest values exceeding 40%, up to a doubling of the current ratio. (The percentage of dry years for SPEI 3, for example, rose from 30% for SSP 126 and 7.1% for SSP 585 over the period 2021-2040 to 72.5% for SSP 126 and 92.1% for SSP 585 over the period 2081-2100). The important role of temperature increase has also been found in terms of increased aridity due to the substantial increase in evapotranspiration ([Waha et al., 2017](#), [Driouech et al., 2020](#)). Land surface feedbacks tend to increase dryness by contributing to increased warming ([Russo et al., 2019](#)).

Our results are consistent with various studies that consistently projected West African countries to become global drought hotspots by the end of the first twenty-first century ([Waha et al., 2017](#), [Almazroui et al., 2020](#)). Variation in future drought changes by methodology has also been highlighted ([Trenberth et al., 2014](#)) with broader agreement on the increase in extreme droughts. The effect of warming on drought severity was detected using the SPEI, which is consistent with the findings of previous studies ([Cook et al., 2018](#)). Our results are also consistent with several studies that indicate an increase in extreme drought conditions around Senegal ([Mbaye et al., 2019](#), [Sadio et al., 2020](#), [Diakhaté et al., 2022](#)).

Although many studies have been conducted on droughts in Senegal ([Faye et al., 2015](#), [Faye et al., 2017](#), [Faye, 2017 & 2018](#)) and on climate projections ([Mbaye et al., 2019](#), [Sadio et al., 2020](#), [Diakhaté](#)

et al., 2022), the projection of events is rare, and using CMIP6 models. Some studies have found that changes in precipitation and temperature could drive the occurrence, frequency and severity of droughts in different contexts, which is consistent with the findings of this work (Sun et al., 2019). (Shiru et al., 2020) used SPEI methods for future (2021-2050 and 2071-2100) drought projection under RCP 2.6, 4.5 and 8.5 in Nigeria, and found that the increase in the drought event could be more evident using the SPEI, and there would be an increase in the frequency and severity of drought, particularly in the semi-arid and arid regions of northern Nigeria, where rainfall is low over the period 2050-2100. This study also suggested that droughts would be more severe under RCP 2.6 and that the frequency of occurrence would be higher, as indicated by the decreasing return period aPETr mid-century.

6. Conclusion

This paper examined the trend in annual precipitation and annual temperature in the Casamance upstream of Kolda and Kayanga upstream of Wassadou catchments over the observation period 1985-2014 and the future period 2015-2100 using CMIP6 projections under SSP 126 and SSP 585. It also assessed the monthly regime of the SPEI, SPI and SSI over the same periods. Over the 8 10-year periods, precipitation will decrease and temperature will increase in both catchments. By 2100 and according to the SSP 126 and SSP 585 emissions scenarios, annual precipitation is expected to be characterised by high variability, while a significant upward trend is forecast for annual temperature (warmer future climate). For each of the two basins, and according to the two emissions scenarios, a decrease in precipitation regardless of the emissions scenario considered. These considerable changes in monthly precipitation in the northern part are expected to occur overall during the dry season, indicating potential extreme events. Given the projected trends and patterns for precipitation and temperature, a decrease in the PIEPS will be noted in the basins as a result of climate change. This is particularly pronounced in the Kayanga to Wassadou basin, where temperatures may be high, which could lead to a decrease in the IPPS, SPI and SSI in all SSPs. However, a combined effect of precipitation and temperature is likely to be important in the two basins where precipitation would decrease significantly during the wintering period under SSP 585, and therefore, the greatest decrease in the SPEI, SPI and SSI. It should be noted that the decrease in SPEI values would not be high compared to areas where temperature is the only determinant, affecting SPEI. In general, a downward trend in the SPEI, SPI and SSI for all seasons was found to be strongly correlated with the upward trend in temperature, suggesting that droughts will be more frequent in both basins under different SSPs. Over the last 20 years of the century, droughts would be less frequent under SSP 126. This may be due to the stabilisation of rising temperatures. The northern regions, where precipitation is low and groundwater is diminishing rapidly, would be the most affected by droughts in all SSPs. The results thus reinforce the observations of previous work, according to which climate variability can increase the frequency and intensity of droughts in Senegal. The methodology developed in this study can be used for reliable projections of drought characteristics in any basin, and the results can be used in the development of adaptation and mitigation plans in Senegal. Future agricultural management strategies should also take possible future conditions into account.

References

- Abbas A., Waseem M., Ullah W., et al., (2021) Spatiotemporal analysis of meteorological and hydrological droughts and their propagations. *Water* 13, 2237. <https://doi.org/10.3390/w13162237>.
- Abramowitz M., and Stegun I.A. (Eds.), (1965) *Handbook of Mathematical Functions with Formulas, Graphs, and Mathematical Tables*. Dover Publications Inc., New York, 1046 p.

- Almazroui M., Saeed F., Saeed S., *et al.*, (2020) Projected change in temperature and precipitation over Africa from CMIP6. *Earth Syst Environ.*, 4, 455–475, <https://doi.org/10.1007/s41748-020-00161-x>
- Ardoïn-Bardin S. (2004) Variabilité hydroclimatique et impacts sur les ressources en eau de grands bassins hydrographiques en zone soudano sahélienne. Thèse de doct. Univ. Montpellier II. 440 p.
- Bae S., Lee S.H., Yoo S.H., Kim T. (2018) Analysis of Drought Intensity and Trends Using the Modified SPEI in South Korea from 1981 to 2010. *Water* 2018, 10, 327. <https://doi.org/10.3390/w10030327>.
- Barker L.J., Hannaford J., *et al.* (2016) From meteorological to hydrological drought using standardised indicators. *Hydrol Earth Syst Sci* 20, 2483–2505. <https://doi.org/10.5194/hess-20-2483-2016>
- Beguiría S., Vicente-Serrano S.M., Reig F., Latorre B. (2014) Standardized precipitation evapotranspiration index (SPEI) revisited, Parameter fitting, evapotranspiration models, tools, datasets and drought monitoring. *Int. J. Climatol.*, 34, 3001–3023.
- Beguiria S., Lattore B., Reig F., and Vicente-Serrano, S. M. (2019) In regards to the SPEI.
- Benitez J. B., Domecq R. M., (2014). Analysis of meteorological drought episodes in Paraguay. *Climatic Change*, 127, 15–25.
- Bevacqua A.G., Chaffe P.L.B., Chagas V.B.P., AghaKouchak A. (2021) Spatial and temporal patterns of propagation from meteorological to hydrological droughts in Brazil. *J Hydrol* 603, 126902. <https://doi.org/10.1016/j.jhydrol.2021.126902>
- Butu H.M., Seo Y., Huh J S., (2020) Determining Extremes for Future Precipitation in Republic of Korea Based on RCP Scenarios Using Non-Parametric SPI. *Sustainability* 2020, 12, 963. <https://doi.org/10.3390/su12030963>
- Carvalho D., Pereira S.C., Rocha A. (2020) Future surface temperature changes for the Iberian Peninsula according to EURO-CORDEX climate projections. *Clim. Dyn.* 2020, 56, 123–138. <https://doi.org/10.1007/s00382-020-05472-3>.
- Chen Y., Li X., Huang K., Luo M., Gao M. (2020) High-Resolution Gridded Population Projections for China Under the Shared Socioeconomic Pathways. *Earth's Future* 2020, 8, e2020EF001491.
- Cook B I., Mankin JS., Anchukaitis K J. (2018) Climate change and drought, from past to future. *Curr Clim Change Rep* 4, 164–179. <https://doi.org/10.1007/s40641-018-0093-2>.
- Council A. (2004) AMS statement on meteorological drought. *Bull. Am. Meteor. Soc.*, 85, 771–773.
- Da Silva R., Lamb L.C., Barbosa M.C., (2016) Universality, correlations, and rankings in the Brazilian universities national admission examinations. *Phys Stat Mech Its Appl* 457, 295–306. <https://doi.org/10.1016/j.physa.2016.03.014>.
- Dacosta H. (1989) Précipitations et écoulements sur le bassin de la Casamance, Thèse de doctorat, Université de Cheikh Anta Diop, Dakar, faculté des lettres et sciences humaines, Département de géographie
- Descroix L., Guichard F., Grippa M., *et al.* (2018) Evolution of surface hydrology in the Sahelo-Sudanian strip, an updated review. *Water* 10, 748. <https://doi.org/10.3390/w10060748>.
- Diakhaté M., Mbaye M. L., Camara I., and Barry M. B. (2022) “Projected Changes in the Rainfall Annual Cycle over the Senegal River Basin Using CMIP5 bias-Corrected Simulations.” *American Journal of Environmental Protection*, 10, no. 1, 41-46. [Doi:10.12691/env-10-1-5](https://doi.org/10.12691/env-10-1-5).
- Draper N.R., Smith H. (1998) Applied regression analysis Wiley.
- Driouech, F., ElRhaz K., Moufouma-Okia, W., *et al.* (2020) Assessing Future Changes of Climate Extreme Events in the CORDEX-MENA Region Using Regional Climate Model ALADIN-Climate. *Earth Syst Environ* 4, 477–492 (2020). <https://doi.org/10.1007/s41748-020-00169-3>.
- Du L., Tian Q., Yu T., Meng Q., Jancso T., Udvardy P., Huang Y. (2013) A comprehensive drought monitoring method integrating MODIS and TRMM data. *Int. J. Appl. Earth Obs.*, 23, 245–253.
- Faye C., Sow A.A. *et* Ndong J.B., (2015) Étude des sécheresses pluviométriques et hydrologiques en Afrique tropicale , caractérisation et cartographie de la sécheresse par indices dans le haut bassin du fleuve Sénégal. *Physio-Géo*, 9, 17 à 35.
- Faye C. (2017) Caractéristiques de la Sécheresse au Sénégal, Méthodes d’analyses, Types d’impacts et Modèles de gestion. Publié aux Editions Universitaires Européennes, 233 p.

- Faye C. (2018) Analysis of drought trends in Senegalese coastal zone on different climatic domains (1951-2010). *Anabelle Uniiversiitãtãiii diin Oradea, Seria Geografie XXVIII*, (2//2018). 231-244.
- Faye C., Ndiaye A., et Mbaye I. (2017) Une évaluation comparative des séquences de sècheresse météorologique par indices, par échelles de temps et par domaines climatiques au Sénégal. *Journal. Wat. Env. Sci.*, 1(1), 11 à 28.
- Fowé, T., Yonaba R., Mounirou L A. et al., (2023) From meteorological to hydrological drought, a case study using standardized indices in the Nakanbe River Basin, Burkina Faso. *Nat Hazards* (2023). <https://doi.org/10.1007/s11069-023-06194-5>.
- Fung, K. F., Huang Y.F., Koo, C.H., Soh, Y.W., (2017) Drought forecasting, A review of modelling approaches 2007–2017. *J. Water Clim. Chang.* 2019, 11, 771–799. <https://doi.org/10.2166/wcc.2019.236>.
- Gbohoui Y.P., Paturel J-E., Tazen F. et al., (2021) Impacts of climate and environmental changes on water resources, a multi-scale study based on Nakanbé nested watersheds in West African Sahel. *J Hydrol Reg Stud* 35, 100828. <https://doi.org/10.1016/j.ejrh.2021.100828>.
- González J., Valdés J.B. (2006) New drought frequency index, Definition and comparative performance analysis. *Water Resour. Res.*, 42. <https://doi.org/10.1029/2005WR004308>.
- Huang S., Huang Q., Chang J., Leng G. (2016) Linkages between hydrological drought, climate indices and human activities, a case study in the Columbia River basin. *Int J Climatol* 36, 280–290. <https://doi.org/10.1002/joc.4344>
- Javanmard S., Emamhadi M., BodaghJamali J., Didehvarasl A. (2017) Spatial-Temporal Analysis of Drought in Iran Using SPI During a Long-Term Period. *Earth Sci.* 2017, 6, 15. <https://doi.org/10.11648/j.earth.20170602.12>.
- Jehanzaib M., Shah S. A., Kim J. E., Kim T.W. (2023) Exploring spatio-temporal variation of drought characteristics and propagation under climate change using multi-model ensemble projections. *Nat Hazards* 115, 2483–2503. <https://doi.org/10.1007/s11069-022-05650-y>
- Kendall M., (1975) *Multivariate Analysis*. Charles Griffin & Company, London, 202 p.
- Lee S.H., Yoo S.H., Choi J.Y., Bae S. (2017) Assessment of the impact of climate change on drought characteristics in the Hwanghae plain, North Korea using time series SPI and SPEI, 1981–2100. *Water*, 9, 579. <https://doi.org/10.3390/w9080579>.
- Li J., Wang Y., Li Y. et al., (2021) Relationship between meteorological and hydrological droughts in the upstream regions of the Lancang-Mekong River. *J. Water Clim. Change.* <https://doi.org/10.2166/wcc.2021.445>.
- Lorenzo-Lacruz J., Vicente-Serrano S., González-Hidalgo J. et al. (2013) Hydrological drought response to meteorological drought in the Iberian Peninsula. *Clim Res* 58, 117–131. <https://doi.org/10.3354/cr01177>.
- Lubes-Niel H., Masson J. M., Paturel J. E., Servat E., (1998) Variabilité climatique et statistiques. Etude par simulation de la puissance et de la robustesse de quelques tests utilisés pour vérifier l'homogénéité de chroniques. *Revue des Sciences de l'Eau*, N° 3, 383-408.
- Ma F., Luo L., Ye A., Duan Q. (2019) Drought characteristics and propagation in the Semiarid Heihe River Basin in Northwestern China. *J Hydrometeorol* 20, 59–77. <https://doi.org/10.1175/JHM-D-18-0129.1>.
- Mann H. B. (1945) Nonparametric Tests against Trend, *Econometrica*. 13 (3), 245-259.
- Masih, I., Maskey S., Mussá F. and Trambauer P. (2014) A review of droughts on the African continent, a geospatial and long-term perspective. *Hydrology and Earth System Sciences* 18, 3635–3649.
- Mbaye M. L., Sylla M.B., Tall M. (2019) Impacts of 1.5 and 2.0 °C Global Warming on Water Balance Components over Senegal in West Africa. *Atmosphere*, 10(11), 712. <https://doi.org/10.3390/atmos10110712>
- McKee T. B., Doesken N. J., Kleist J. and coauthors. (1993) The relationship of drought frequency and duration to time scales. In, *Proceedings of the 8th conference on applied climatology*, Boston, pp 179–183.
- Mdehheb Z., Elkihel B., et al. (2020), The Environmental Management System and its application impacts on the business economy in the eastern region of Morocco, *Caspian J. Environ. Sci.* 18(1), 13-20

- Mishra A. K., and Singh, V P. (2010) A review of drought concepts. *Journal of hydrology* 391, 202–216.
- Mohsenipour M., Shahid S., Chung E S. and Wang, X. J. (2018) Changing pattern of droughts during cropping seasons of Bangladesh. *Water resources management* 32, 1555–1568.
- Montes-Vega MJ., Guardiola-Albert C. and Rodríguez-Rodríguez M. (2023) Calculation of the SPI, SPEI, and GRDI Indices for Historical Climatic Data from Doñana National Park, Forecasting Climatic Series (2030–2059) Using Two Climatic Scenarios RCP 4.5 and RCP 8.5 by IPCC. *Water*. 2023; 15(13), 2369. <https://doi.org/10.3390/w15132369>.
- O'Neill B. C., Kriegler E., Ebi K. L., Kemp-Benedict E., Riahi K., Rothman D. S., van Ruijven B. J., Van Vuuren D. P., Birkmann J., Kok K., Levy M. and Solecki, W. (2017) The roads ahead, Narratives for shared socioeconomic pathways describing world futures in the 21st century. *Global Environmental Change*, 42, 169-180, <https://doi.org/10.1016/j.gloenvcha.2015.01.004>
- OMVS. (2012) Plan d'Action GIRE du bassin versant du fleuve Kayanga/Géba Volume 3, Portfolio de projets, Facilité Africaine de l'Eau, 125 p.
- Pettitt A. N. (1979) A non-parametric approach to the change-point problem. *Appl. Statist.*, 28 (2), 126-135. <https://doi.org/10.2307/2346729>
- Potop V., Boroneanț C., Možný M., Štěpánek P. and Skalák, P. (2014) Observed spatiotemporal characteristics of drought on various time scales over the Czech Republic. *Theor. Appl. Climatol.*, 115, 563–581.
- Projet d'Appui au Développement Rural en Casamance (PADERCA). (2008) Etablissement de la situation de référence du milieu naturel en basse et moyenne Casamance. République du Sénégal Ministère de l'Agriculture Rapport final, 201 p.
- Rashid M. M., Beecham S. and Chowdhury, R.K. (2015) Statistical downscaling of CMIP5 outputs for projecting future changes in rainfall in the Onkaparinga catchment. *Science of the Total Environment* 530, 171–182.
- Russo A., Gouveia C.M., Dutra E., Soares P M M., Trigo R. M. (2019) The synergy between drought and extremely hot summers in the Mediterranean. *Environ Res Lett* 14, 014011.
- Sa'adi Z., Shahid S., Chung E-S. and bin Ismail T. (2017) Projection of spatial and temporal changes of rainfall in Sarawak of Borneo Island using statistical downscaling of CMIP5 models. *Atmospheric research* 197, 446–460.
- Saada N., Abu-Romman A. (2017) Multi-site Modeling and Simulation of the Standardized Precipitation Index (SPI) in Jordan. *J. Hydrol. Reg. Stud.*, 14, 83–91. <https://doi.org/10.1016/j.ejrh.2017.11.002>.
- Sadio P.M., Mbaye M.L., Diatta S., Sylla M.B. (2020) Variabilité et changement hydroclimatiques dans le bassin-versant du fleuve Casamance (Sénégal). *La Houille Blanche* 6, 89–96.
- Sagna P. (2005) Dynamique du climat et de son évolution récente dans la partie ouest de l'Afrique occidentale. Thèse de Doctorat d'Etat, Université Cheikh Anta Diop de Dakar, 786 p.
- Sahoo A.K., Sheffield J., Pan M. and Wood, E.F. (2015) Evaluation of the tropical rainfall measuring mission multi-satellite precipitation analysis (TMPA) for assessment of large-scale meteorological drought. *Remote Sens. Environ.*, 159, 181–193.
- Salimi H., Asadi E., Darbandi S. (2021) Meteorological and hydrological drought monitoring using several drought indices. *Appl Water Sci* 11, 11. <https://doi.org/10.1007/s13201-020-01345-6>.
- Salman S.A., Shahid S., Ismail T., Ahmed K., Wang, X-J. (2018) Selection of climate models for projection of spatiotemporal changes in temperature of Iraq with uncertainties. *Atmospheric research* 213, 509–522
- Sané T., Sy O. et Dieye, E.H. B. (2011) Changement climatique et vulnérabilité de la ville de Ziguinchor. Actes du colloque "Renforcer la résilience au changement climatique des villes, du diagnostic spatialisé aux mesures d'adaptation" (2R2CV) 07 et 08 juillet 2011, Université Paul Verlaine - Metz, France, 1-14.
- Sen P.K. (1968) Estimates of the Regression Coefficient Based on Kendall's Tau. *Journal of the American Statistical Association*, 63, 1379-1389.
- Servat E., Paturel J E., Kouame B., Travaglio M., Ouedraogo M., Boyer J. F., Lubes-NieL H., Fritsch J.M., Masson J. M., Marieu B. (1998) Identification, caractérisation et conséquences d'une variabilité hydrologique en Afrique de l'Ouest et centrale. *IAHS Publication*, N°252, 323-337.

- Shiru M. S., Shahid S., Dewan A., Chung E-S., Alias N., Ahmed K. and Hassan, Q.K. (2020) Projection of meteorological droughts in Nigeria during growing seasons under climate change scenarios. *Sci Rep* 10, 10107. <https://doi.org/10.1038/s41598-020-67146-8>
- Sun F., Mejia A., Zeng P. and Che Y. (2019) Projecting meteorological, hydrological and agricultural droughts for the Yangtze River basin. *Science of the Total Environment* 696, 134076 (2019).
- Thorntwaite C.W. (1948) An approach toward a rational classification of climate. *Geogr. Rev.*, 55–94.
- Törnros T., Menzel L. (2014) Addressing drought conditions under current and future climates in the Jordan River region. *Hydrol. Earth Syst. Sci.*, 18, 305–318.
- renberth K.E et al. (2014) Global warming and changes in drought. *Nat Clim Chang.* 4, 17–22. <https://doi.org/10.1038/nclimate2067>.
- Van Vuuren D.P., Edmonds J., Kainuma M., Riahi K., Thomson, A., Hibbard K., Hurtt G.C., Kram T., Krey V., Lamarque J-F. et al. (2011) The representative concentration pathways, An overview. *Clim. Chang.*, 109, 5–31. <https://doi.org/10.1007/s10584-011-0148-z>
- Vicente-Serrano S. M., Beguería S., López-Moreno J.I. (2010) A multiscale drought index sensitive to global warming, the standardized precipitation evapotranspiration index. *J. Clim.* 23, 1696–1718. <https://doi.org/10.1175/2009JCLI2909.1>
- Waha K. et al. (2017) Climate change impacts in the Middle East and Northern Africa (MENA) region and their implications for vulnerable population groups. *Reg Environ Change* 17, 1623–1638.
- Wan Zunairah O. and Nurul Nadrah A. T. (2023) Assessment on the Climate Change Impact Using CMIP6. Published under licence by IOP Publishing Ltd, IOP Conference Series, *Earth and Environmental Science*, 1140, DOI 10.1088/1755-1315/1140/1/012005.
- Wang F., Wang Z., Yang H. et al. (2020) Comprehensive evaluation of hydrological drought and its relationships with meteorological drought in the Yellow River basin, China. *J. Hydrol.* 584, 124751. <https://doi.org/10.1016/j.jhydrol.2020.124751>.
- Wu J., Chen X., Yao H. et al. (2017) Non-linear relationship of hydrological drought responding to meteorological drought and impact of a large reservoir. *J. Hydrol.* 551, 495–507. <https://doi.org/10.1016/j.jhydrol.2017.06.029>
- Wu J., Liu Z., Yao H. et al. (2018) Impacts of reservoir operations on multi-scale correlations between hydrological drought and meteorological drought. *J. Hydrol.* 563, 726–736. <https://doi.org/10.1016/j.jhydrol.2018.06.053>.
- Xing L., Binbin H., Xingwen Q., Zhanmang L. and Xiaojing B. (2015) Use of the Standardized Precipitation Evapotranspiration Index (SPEI) to Characterize the Drying Trend in Southwest China from 1982–2012. *Remote Sens*, 7, 10917-10937.
- Yevjevich V. (1967) An Objective Approach to Definitions and Investigations of Continental Hydrologic Drought; Hydrology Paper No. 23; Colorado State University, Fort Collins, CO, USA.
- Yonaba R., Mounirou LA., Tazen F. et al. (2023) Future climate or land use? Attribution of changes in surface runoff in a typical Sahelian landscape. *C R Géosci.* 355, 1–28. <https://doi.org/10.5802/crgeos.179>
- Zeybekoğlu U., Aktürk G. A. (2021) comparison of the China-Z Index (CZI) and the Standardized Precipitation Index (SPI) for drought assessment in the Hirfanli Dam basin in central Turkey. *Arab. J. Geosci.* 2021, 14, 2731. <https://doi.org/10.1007/s12517-021-09095-8>.
- Zhang A. and Jia G. (2013) Monitoring meteorological drought in semiarid regions using multi-sensor microwave remote sensing data. *Remote Sens. Environ.*, 134, 12–23.

(2024): <http://www.jmaterenvirosci.com>